THE APPLICATION OF POST-HOC CORRECTION METHODS FOR SOFT TISSUE ARTIFACT AND MARKER MISPLACEMENT IN YOUTH GAIT KNEE KINEMATICS

A Thesis

presented to

the Faculty of California Polytechnic State University,

San Luis Obispo

In Partial Fulfillment

of the Requirements for the Degree

Master of Science in Mechanical Engineering

by

Kaila Lawson

June 2021

COMMITTEE MEMBERSHIP

TITLE:	The Application of Post-Hoc Correction Methods for Soft Tissue Artifact and Marker Misplacement in Youth Gait Knee Kinematics
AUTHOR:	Kaila Lawson
DATE SUBMITTED:	June 2021
COMMITTEE CHAIR:	Stephen Klisch, Ph.D. Professor of Mechanical Engineering
COMMITTEE MEMBER:	Scott Hazelwood, Ph.D. Professor of Biomedical Engineering
COMMITTEE MEMBER:	Britta Berg-Johansen, Ph.D. Professor of Biomedical Engineering

ABSTRACT

The Application of Post-Hoc Correction Methods for Soft Tissue Artifact and Marker Misplacement in Youth Gait Knee Kinematics

Kaila Lawson

Biomechanics research investigating the knee kinematics of youth participants is very limited. The most accurate method of measuring knee kinematics utilizes invasive procedures such as bone pins. However, various experimental techniques have improved the accuracy of gait kinematic analyses using minimally invasive methods. In this study, gait trials were conducted with two participants between the ages of 11 and 13 to obtain the knee flexion-extension (FE), adduction-abduction (AA) and internal-external (IE) rotation angles of the right knee. The objectives of this study were to (1) conduct pilot experiments with youth participants to test whether any adjustments were necessary in the experimental methods used for adult gait experiments, (2) apply a Triangular Cosserat Point Element (TCPE) analysis for Soft-Tissue Artifact (STA) correction of knee kinematics with youth participants, and (3) develop a code to conduct a Principal Component Analysis (PCA) to find the PCA-defined flexion axis and calculate knee angles with both STA and PCA-correction for youth participants. The kinematic results were analyzed for six gait trials on a participant-specific basis. The TCPE knee angle results were compared between uncorrected angles and another method of STA correction, Procrustes Solution, with a repeated measures ANOVA of the root mean square errors between each group and a post-hoc Tukey test. The PCA-corrected results were analyzed with a repeated measures ANOVA of the FE-AA correlations from a linear regression analysis between TCPE, PS, PCA-TCPE and PCA-PS angles. The results indicated that (1) youth experiments can be conducted with minor changes to experimental methods used for adult gait experiments, (2) TCPE and PS analyses did not yield statistically different knee kinematic results, and (3) PCA-correction did not reduce FE-AA correlations as predicted.

Keywords: Soft Tissue Artifact, Triangular Cosserat Point Element, Principal Component Analysis, Knee kinematics

ACKNOWLEDGMENTS

Thank you to my thesis committee, Dr. Stephen Klisch, Dr. Scott Hazelwood and Dr. Britta Berg-Johansen for the continued advice and guidance. Thank you to my family and friends for the love and support throughout this journey. A special thank you to Samuel Tucker for the endless encouragement and mentorship on this project.

TABLE OF CONTENTS

Page

LIST OF TABLES

LIST OF FIGURES

Chapter 1
INTRODUCTION

Gait kinematics of adults is a well-researched topic in the biomechanics field. Studies have established ranges of knee angles for adults with normal gait, in addition to various conditions which may affect gait patterns [1-14]. People who are overweight or obese tend to have different gait patterns than people who are normal weight [2], [8]. Additionally, these changes in gait kinematics due to overweight and obesity may lead to an increased risk of the development of osteoarthritis of the knee [11], [12]. However, research regarding gait kinematics in children and the effects of childhood obesity on knee angles is limited. The long-term goal of this study is to analyze differences in gait depending on the weight category in youth to determine the risk factors of osteoarthritis as well as possible mitigation of risk by intervention methods such as diet and exercise programs.

Given that children are classified as a vulnerable population in human subject research, the importance of minimal risk is particularly significant. The use of surface-mounted retroreflective markers to record gait kinematics is a simple solution for risk minimization. However, markers placed on the skin are susceptible to experimental errors that affect knee angle calculations due to soft tissue artifact and marker misplacement [15-16]. Soft tissue artifact (STA) is caused by the movement of skin and adipose tissue relative to the underlying bone segment. The use of skin-mounted markers yields results susceptible to errors up to 10, 50 and 100% for flexion-extension, adduction-abduction, and internal-external rotation angles, respectively [17]. Marker misplacement is another source of error in gait kinematic analysis with skin markers and can occur despite careful attempts at placement, especially for participants with greater amounts of adipose tissue. The accurate placement of markers is critical since the medial and lateral knee markers often define the knee flexion axis, which is crucial for knee joint kinematics analysis [18]. While placement of the knee markers superiorly or inferiorly of the anatomical position will not greatly affect the results, an anteriorly or posteriorly placed marker can lead to significant changes in the patterns of the knee angle results [18]. These errors can lead to an increase in the correlation between flexion and adduction angles, known as crosstalk

[19]. Mitigation of these errors is crucial for studying knee kinematics and the ability to identify differences in gait between populations.

While soft tissue artifact and marker misplacement are concerns, post-hoc methods to improve the accuracy of the knee kinematics have been developed [18], [20–24]. The most common bone pose estimation technique to correct for STA uses Procrustes Solution (PS) to measure shape change in skin-mounted markers to predict the rigid motion of the bone segments [20], [25]. Another method of STA correction utilizes Triangular Cosserat Point Elements (TCPE) from marker clusters on the thigh and shank segments to distinguish STA from the rigid-body motion of the segments by individually calculating strain, relative rotation and relative translation of each TCPE [21]. Filtering parameters are used to determine the TCPEs that best predict the rigid body motion of the underlying bone segments. The rotation tensors of these TCPEs are then applied to the thigh and shank segments throughout time to calculate the knee angles with STA correction [21]. A post-hoc correction method for marker misplacement uses principal component analysis (PCA) to identify a motion-based, rather than marker-based, knee-flexion axis [18]. This PCA-corrected flexion axis is then used to define the knee-coordinate system with which the corrected knee angles are calculated.

Methods that improve the accuracy of the knee kinematics are useful. However, the application of these methods with youth participants is minimal. Without significant documentation of the use of these two methods with children, it is not yet known if any complexities arise in the procedure or analyses with youth participants. The main goals of this study were to (1) conduct pilot experiments to test whether any adjustments were necessary in the experimental methods for youth participants vs. adult participants, (2) apply a TCPE analysis for STA correction of knee kinematics with youth participants, and (3) develop a code to conduct a PCA analysis to find the PCA-defined flexion axis and calculate knee angles with both STA and PCA-correction for youth participants.

The hypotheses for this study were that (1) gait experiments with youth participants could be conducted with minor changes to the experimental procedures that are used for adult gait experiments, (2) the TCPE knee angle results would not differ from the PS knee angle results

since the two methods of STA-correction are similar, but both PS and TCPE knee angles would differ from the knee angles without STA correction, (3) PCA correction would decrease the correlation between the FE-AA angles. In order to test the hypotheses, (1) any changes in the procedure from the adult gait experiments were noted, (2) the root mean square error (RMSE) was calculated between each method of the TCPE analysis (TCPE, PS, Uncorrected), a repeated measures ANOVA was conducted on the RMSE values to test for differences between groups and a post-hoc Tukey test was conducted to test which groups differed, (3) a linear regression analysis was conducted on the FE-AA angles and a repeated measures ANOVA was conducted on the R^2 values for PS, TCPE, PCA-corrected PS and PCA-corrected TCPE angles.

Chapter 2

METHODS

2.1 Data Collection

2.1.1 Participant Consent

Experimental protocols were approved by Cal Poly's Institutional Review Board and were designed to minimize risk to human subjects. Gait experiments were conducted in Cal Poly's Human Motion Biomechanics lab with two normal weight (1 female, 1 male) youth participants, ages 11- and 13-years old. Table 2.1 contains height, mass and BMI of the participants. Participants were informed of the gait experiment process and written consent was received from the participants and a parent. Each participant selected a Human Motion Biomechanics Laboratory staff member with which they felt most comfortable applying the retroreflective markers and consented to contact for the application.

Table 2.1 : Youth participant information.

Participant	Age	Gender	Height [cm]	Mass [kg]	BMI
1	13	M	162	52.45	20.0
2	11	F	143.5	35	17.0

2.1.2 Retroreflective Marker Placement

Forty-four (44) retroreflective markers were placed on the participants on anatomical landmarks in the modified Enhanced Helen Hayes (HH) marker set and the Triangular Cosserat Point Element (TCPE) marker set. The Enhanced HH marker set consists of 32 markers: crown of the head, acromion processes, 7th cervical vertebra, sternum, posterior superior iliac spines, sacrum, anterior superior iliac spines, greater trochanters, anterior thighs, lateral and medial epicondyles, head of fibulae, tibial tuberosities, anterior shanks , lateral and medial malleoli, heel at Achilles tendon insertion, and both feet between 3rd and 4th metatarsals (Fig. 2.1). The remaining 12 markers were strategically placed on the right leg: six on the anterior/lateral thigh and six on the anterior/lateral shank (Fig. 2.2). These twelve markers were placed with regards to

the placement of the existing thigh and shank markers from the modified Enhanced HH marker set to avoid any 3-marker collinearities. The six additional markers plus the modified Enhanced HH thigh or shank marker formed the 7-marker clusters on the thigh and shank segments utilized in the TCPE analysis (Fig. 2.3).

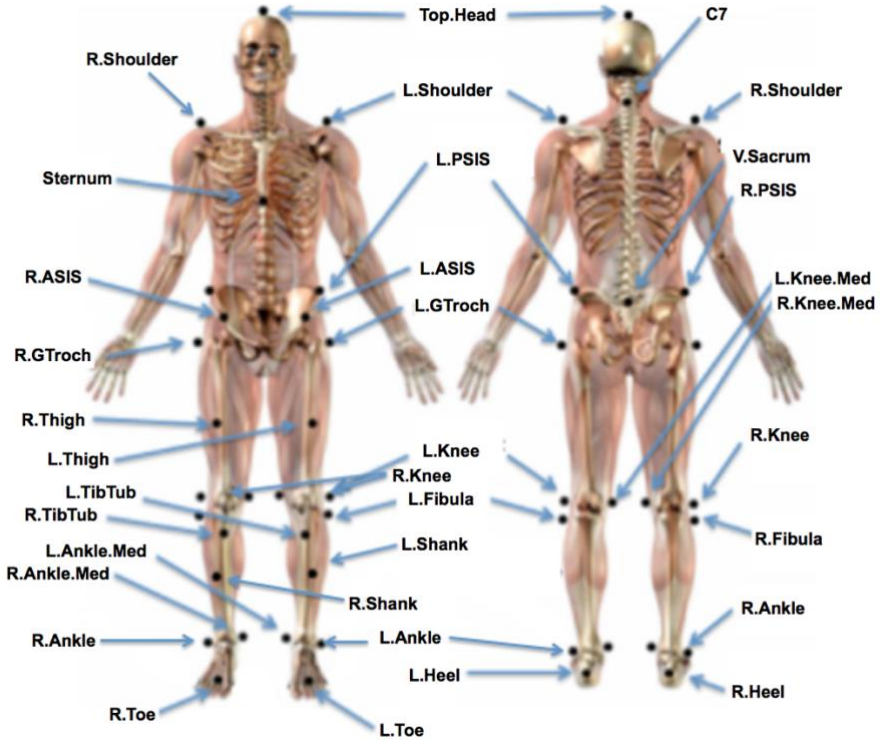

Figure 2.1: The anatomical positions of the modified Enhanced Helen Hayes markers. [26]

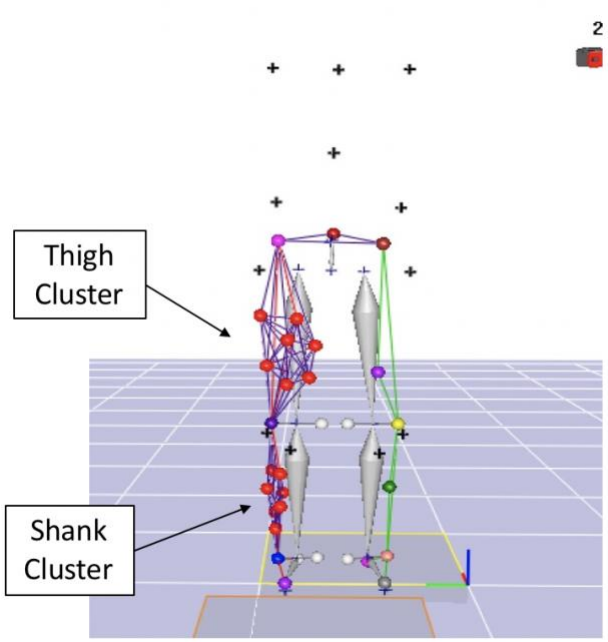

Figure 2.2: The Triangular Cosserat Point Element marker set (red markers) post-processed in Cortex Motion Analysis Software.

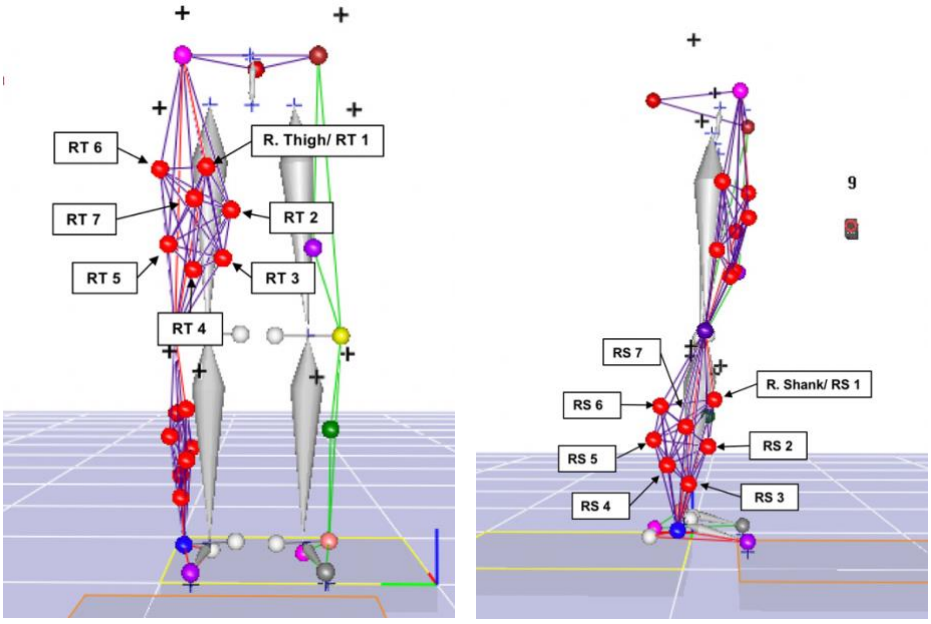

Figure 2.3 (Left) The marker identification of the right leg thigh marker cluster in Cortex from the anterior perspective. (Right) The marker identification of the right leg shank marker cluster from the lateral perspective.

2.1.3 Gait Experiments

Gait trials were recorded using a 12-camera motion analysis system with Cortex software (Motion Analysis Corp., Santa Rosa, CA, USA) at a frequency of 150Hz. The Cortex cameras record the position (x-, y-, z-coordinates) of the retroreflective markers throughout time. The static trials were conducted first with the participant standing on a marked location on the floor with their feet hip-width apart in a comfortable, natural stance and arms bent and lifted (Fig. 2.4). A one-second recording was collected, and the participant was then asked to take a few steps away from the marked location before returning and assuming the static pose positioning again. This process was repeated until five static trials were recorded. The medial markers and the top of the head marker were removed following the static trials.

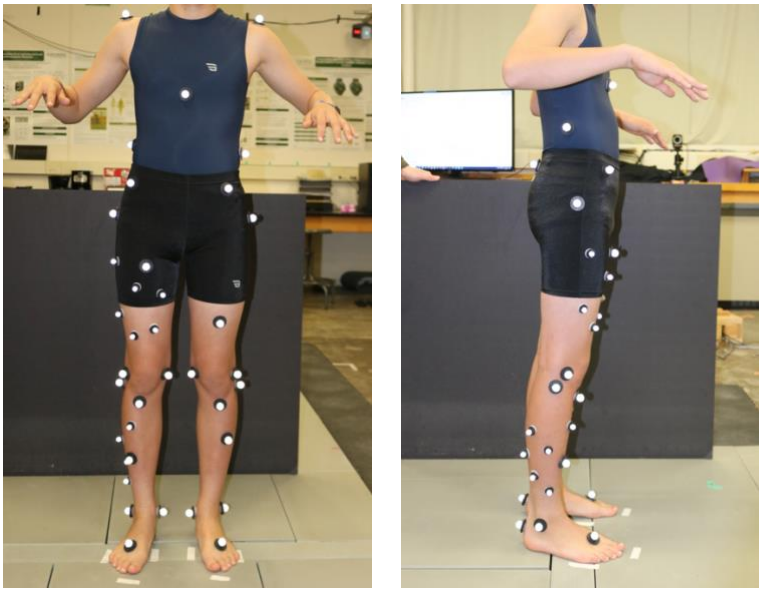

Figure 2.4: Static pose with the Enhanced HH and TCPE marker sets.

The gait walkway containing four force plates (Accugait, AMTI, Watertown, MA, USA) was adjusted for youth participants by decreasing the spacing between each force plate to account for the decreased stride length of youth participants. Before recording dynamic trials, it was ensured that the participants were able to make foot contact with each force plate while walking, beginning with the left foot on the first force plate. Dynamic trials were then conducted by recording the participant walking at a self-selected walking speed along the platform of the four

force plates recorded at a 150Hz frequency (Fig. 2.5). This procedure was repeated for each participant until six satisfactory dynamic trials were recorded.

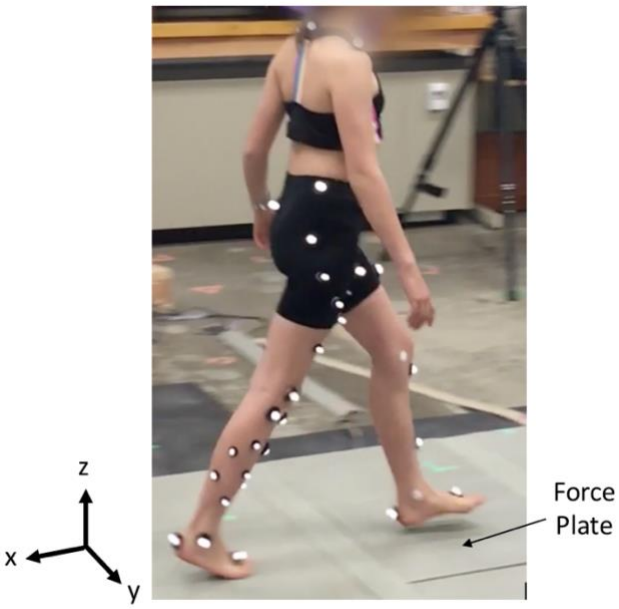

Figure 2.5: A participant walking across the gait platform during a dynamic trial with the definition of the global coordinate system. The direction of gait occurs in the negative x-direction.

2.2 Data Post-Processing

Post-processing of the marker data was performed using Cortex motion analysis software. One static trial and six dynamic trials were post-processed per participant. The modified Enhanced HH markers were labelled according to anatomical positions and the TCPE markers were numbered, one through seven, for both the thigh and shank segments. The Enhanced HH right thigh marker and right shank markers were labeled as the first TCPE thigh cluster and shank cluster markers, respectively (Fig. 2.3). Selected trials were inspected for any uncaptured or misidentified markers and were manually corrected to ensure correct marker labeling was recorded. For the dynamic trials, the marker data was filtered using a 4th-order Butterworth filter with a 6Hz cutoff frequency. The marker data consists of the x-, y-, z-coordinates of each marker as a function of time in the global coordinate system, where the negative x-direction is along the gait platform in the direction of gait, the z-direction is toward the ceiling, and y-direction is the

cross product of z and x (i.e. pointing towards the right of the participant during gait trials). The marker data were saved for one static trial and six dynamic trials for each participant. Cortex calculates knee flexion-extension (FE), abduction-adduction (AA), and internal-external (IE) angles from the marker positioning throughout time and these angles were saved and will be referred to as the uncorrected (UC) knee angles with which to compare knee angles following STA methods.

2.3 Knee Angle Correction Methods

2.3.1 Triangular Cosserat Point Element (TCPE) Method Correction

The method of STA correction with Triangular Cosserat Point Elements is based on the theory outlined by Solav and the equations presented in this section were established by Solav [21]. The implementation of the TCPE method was conducted by importing the post-processed marker data and force plate data from Cortex into a MATLAB code written previously [27], [28]. The code follows the theory of Solav but has algorithmic differences based on assumptions made. The first difference is the use of 7 markers for the clusters rather than 12 markers used by Solav. Secondly, equal weightings of the translation, rotation and strain filtering parameters were assumed and implemented in the TCPE code.

The marker clusters on the thigh and shank segments were used for the TCPE analysis by creating each possible combination of three markers for a total of 35 TCPE's for each segment. This method analyzes the strain, relative rotation and relative translation of each of the TCPE's and utilizes filtering parameters to identify the TCPE's that best predict the rigid body motion of the underlying bone segment for a gait cycle. A gait cycle is defined as heel strike to heel strike of the right foot, which occurs at the first non-zero reading of the second and fourth force plates (Fig. 2.6).

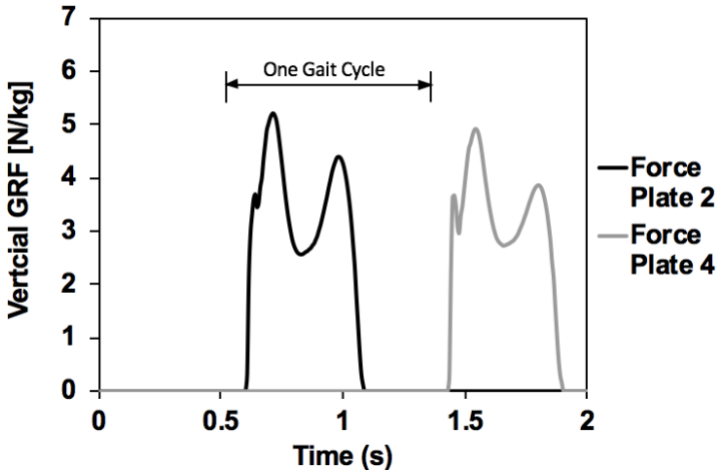

Figure 2.6: Force plate readings of ground reaction force (GRF) of the second and fourth force plates. One gait cycle spans from the first signal of the second force plate to the first signal of the fourth force plate.

Direction vectors were created from each TCPE for the static pose, used as the reference configuration, and for the dynamic trials at each time point. The present configuration direction vector, $\boldsymbol{d}_i$, and the reciprocal of the reference configuration direction vector, $\boldsymbol{D}^i$, were used to calculate the deformation gradient tensor, $\boldsymbol{F}$, for each TCPE at each time point in the dynamic trial using equation (1).

$$\boldsymbol{F} = \boldsymbol{d}_i \otimes \boldsymbol{D}^i \tag{1}$$

Using polar decomposition, the deformation gradient tensor can be multiplied by the inverse of the stretch tensor, **M**, to solve for the rotation tensor, **R** (Eqn 2).

$$\boldsymbol{R} = \boldsymbol{F}\boldsymbol{M}^{-1} \tag{2}$$

In order to compute the strain in the TCPE's, the Lagrangian strain tensor, **E**, was calculated using equation (3), where **C** is the right Cauchy-Green deformation tensor and **I** is the identity tensor.

$$\boldsymbol{E} = \frac{1}{2}\boldsymbol{C} - \boldsymbol{I} = \frac{1}{2}\boldsymbol{F}^T\boldsymbol{F} - \boldsymbol{I} \tag{3}$$

The translation of each TCPE was calculated between the centroid of a TCPE and a reference point — the knee joint center (KJC). The translation of this reference point was calculated as the difference in the present and reference configuration vectors, $\boldsymbol{x}^{(B)}$ and $\boldsymbol{X}^{(B)}$, respectively. The present configuration vector, $\boldsymbol{x}^{(B)}$, was calculated from the present configuration

TCPE centroid, $\bar{\boldsymbol{x}}$, minus the deformed difference between the static configuration centroid, $\bar{\boldsymbol{X}}$, and reference configuration vector, $\boldsymbol{X}^{(B)}$ (Eqn. 4).

$$\boldsymbol{t}^{(B)} = \boldsymbol{x}^{(B)} - \boldsymbol{X}^{(B)} = \bar{\boldsymbol{x}} - \boldsymbol{F}\left(\bar{\boldsymbol{X}} - \boldsymbol{X}^{(B)}\right) - \boldsymbol{X}^{(B)} \tag{4}$$

The relative rotation of a TCPE was found by first calculating the relative angle between each combination of two TCPEs where the relative angle, $\phi_{j/k}$, between the *j* and *k*th TCPE is:

$$\phi_{j/k} = cos^{-1}\left[\frac{1}{2}(\boldsymbol{R}_j \cdot \boldsymbol{R}_k - 1)\right] \tag{5}$$

where $\mathbf{R}_j$ and $\mathbf{R}_k$ are the rotation tensors of the *j* and *k*th TCPE, respectively. The relative angle of the *j*th TCPE relative to all TCPEs at one time point is shown in equation (6), where N is the total number of TCPEs.

$$\phi_j = \frac{1}{N-1}\sum_{k=1}^{N} \phi_{j/k} \tag{6}$$

The translation of the *j*th TCPE relative to the translation of all the TCPEs can be calculated from the translation of the *j* and *k*th translation vectors, $\mathbf{t}_j^{(B)}$ and $\mathbf{t}_k^{(B)}$ (Eq. 7).

$$T_j = \frac{1}{N-1}\sum_{k=1}^{N}\left|\boldsymbol{t}_j^{(B)} - \boldsymbol{t}_k^{(B)}\right| \tag{7}$$

The magnitude of the strain tensor of the jth TCPE was calculated from equation (8).

$$E_j = \sqrt{\boldsymbol{E}_j \cdot \boldsymbol{E}_j} \tag{8}$$

The relative rotation, relative translation and strain were normalized by their respective ranges of magnitude to yield the parameters N_ϕ, N_T, and N_E, representing normalized rotation, normalized translation and normalized strain, respectively. The average of the three parameters yields the combined normalized filtering parameter, $N_{combined}$, calculated in equation (9).

$$N_{combined} = (N_\phi + N_T + N_E)/3 \tag{9}$$

A canonical extension of Solav's filtering algorithm was used. If the normalized filtering parameter was less than or equal to 0.1, a TCPE was considered a good estimate of the motion of the underlying bone segment. The TCPEs which meet this criterion were selected and their rotation tensors were averaged in order to get the best predicted rotation tensor for each time

point. If no TCPEs met the criterion, the three TCPEs with the lowest normalized filtering parameters were selected.

The flexion, adduction and internal rotation angles of the right knee throughout a gait cycle were calculated as outlined by Grood [29] using a floating axis coordinate system. The thigh and shank segments have distinct body-fixed coordinate systems defined from anatomical locations (Fig. 2.7). These axes were estimated in the TCPE code from the markers. The Z-axis of the thigh segment was calculated from the KJC to the hip joint center (HJC). This vector will subsequently be referred to as the thigh vector. The Y-axis of the thigh was calculated as the cross product of the Z-axis and a temporary vector from the medial to lateral knee marker. The X-axis was the cross product of the Y- and Z-axes. The shank coordinate system was defined with the z-axis from the ankle joint center (AJC) to the KJC, the y-axis as the cross product of the z-axis with a vector pointed from the medial to lateral ankle marker, and the x-axis as the cross product of the y- and z-axes.

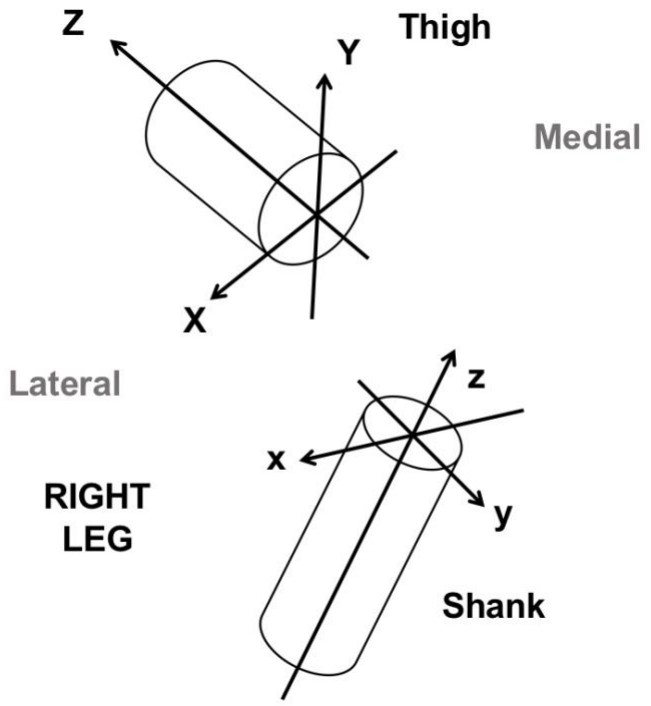

Figure 2.7: The thigh and shank segment fixed body coordinate systems.

In the floating axis coordinate system described by Grood, the axis about which FE occurs is the X-axis of the thigh, the axis about which IE rotation occurs is the z-axis of the shank, and AA occurs about a floating axis, $\mathbf{e}_2$, calculated from the normalized cross product of the IE and FE axes (Fig. 2.8). The normalized thigh axes are referred to as **I**, **J** and **K**, and the normalized shank axes are referred to as **i**, **j** and **k**.

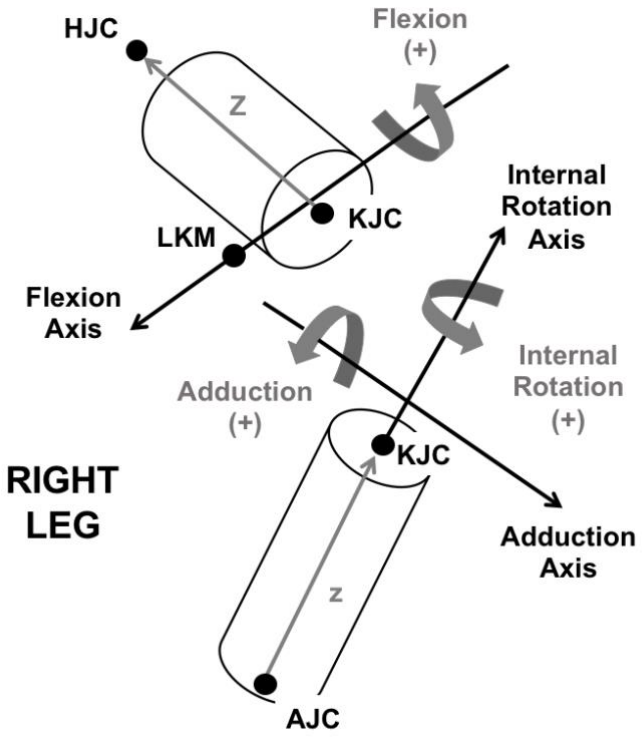

Figure 2.8: The definition of FE, AA and IE with the floating axis coordinate system.

The FE angle, α, was calculated with the floating axis, $\mathbf{e}_2$, and the thigh vector, **K**, from equation (10). The AA angle, β, was calculated using the thigh segment axis, **I**, and the shank segment axis, **k** in equation (11). Equation (12) shows the calculation of the IE angle, γ, using $\mathbf{e}_2$, the floating axis, and the shank segment axis, **i**.

$$\alpha = sin^{-1}(-\boldsymbol{e}_2 \cdot \boldsymbol{K}) \tag{10}$$

$$\beta = -\left(cos^{-1}(\boldsymbol{I} \cdot \boldsymbol{k}) - \frac{\pi}{2}\right) \tag{11}$$

$$\gamma = -sin^{-1}(-\boldsymbol{e}_2 \cdot \boldsymbol{i}) \tag{12}$$

The angles are positive in flexion, abduction, and external rotation as defined by Grood [29]. However, in this study, adduction and internal rotation will be considered positive, which have been reflected in equations (11) and (12) by the negative signs.

2.3.2 Principal Component Analysis (PCA) Method Correction

The principal component analysis for correction of the knee flexion axis follows the procedure established by [18] and was implemented with a custom function written in MATLAB (MathWorks, Natick, MA, USA). The three-dimensional marker coordinates of the HJC, KJC, lateral right knee, and lateral right ankle were imported into the MATLAB function to perform the PCA analysis. The HJC and KJC markers were virtual markers calculated by Cortex from the Enhanced HH marker set. The virtual right KJC was calculated by Cortex relative to the right knee, right ankle and shank markers. The virtual right HJC was calculated relative to the right ASIS, sacrum and the midpoint of the left and right ASIS. The coordinates of these virtual markers were used to define the vector from the KJC to the HJC, representing the thigh vector. A virtual, transverse plane was created perpendicular to the thigh vector and in-plane with the lateral knee marker (Fig. 2.9). Since the KJC does not necessarily lie within this plane, the point at which the thigh vector intersects with the transverse plane will be referred to as point *A*. A coordinate system in the plane was established using *A* as its origin, with the vectors $\mathbf{v_1}$ and $\mathbf{v_2}$ as its basis. The vector $\mathbf{v_1}$ is defined as a unit vector pointing from *A* to the lateral knee marker, representing the marker-based FE axis. The second basis vector, $\mathbf{v_2}$, is defined as the cross product of the normalized thigh vector and $\mathbf{v_1}$, as shown in equation (13).

$$v_2 = \widehat{thigh\_vector} \times v_1 \tag{13}$$

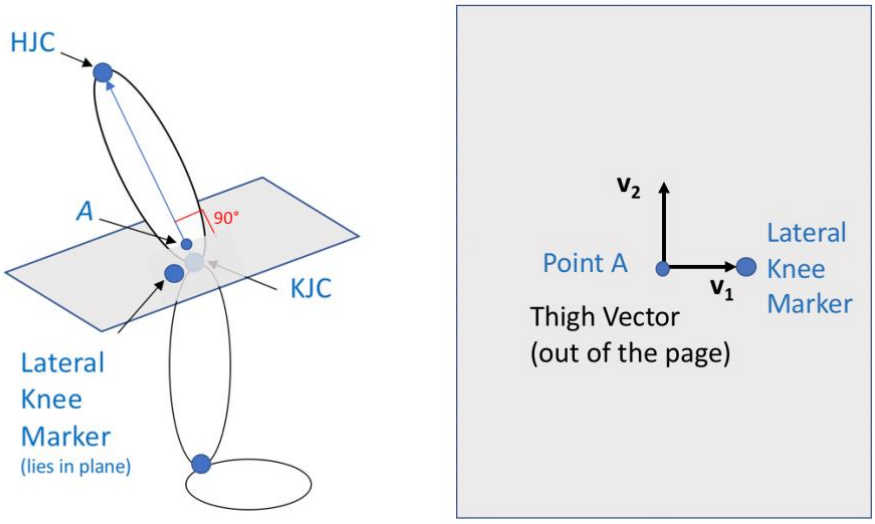

Figure 2.9: (Left) The transverse plane perpendicular to the thigh vector and in plane with the lateral knee marker. (Right) The top view of the transverse plane with basis vectors $\mathbf{v_1}$ and $\mathbf{v_2}$.

The lateral ankle marker was projected onto the plane, where its position vector was described using the coordinate system at *A,* in terms of the basis vectors $\mathbf{v_1}$ and $\mathbf{v_2}$ (Fig. 2.10). The vectors $\mathbf{v_1}$, $\mathbf{v_2}$ and the thigh vector can be used to describe the thigh segment coordinate system. Next, the projection of the ankle marker was plotted throughout the gait motion, creating a two-dimensional system of points (Appendix A).

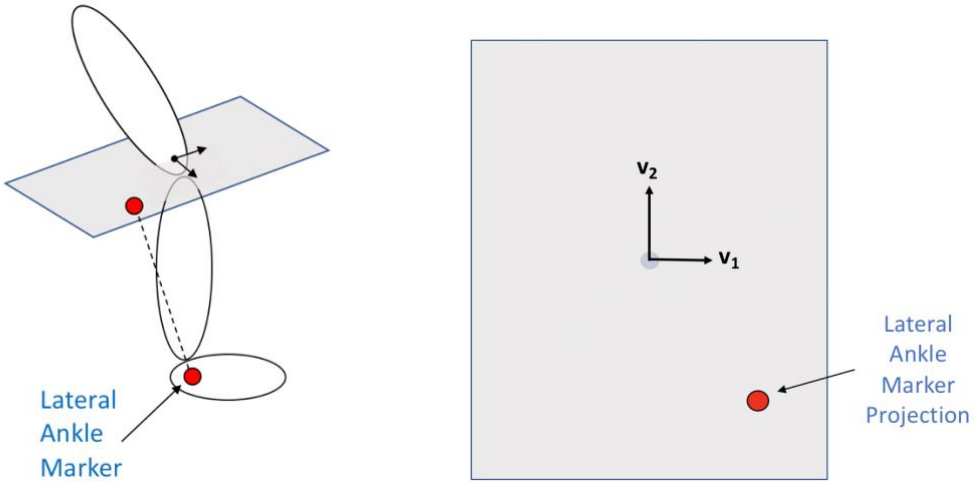

Figure 2.10: (Left) Lateral ankle marker projection onto the transverse plane. (Right) Top view of the transverse plane with one time point of the lateral ankle marker projection.

The PCA analysis was conducted on the 2-D dataset created on the transverse plane. The covariance matrix was calculated for the dataset and was diagonalized in order to find the eigenvalues. The greatest eigenvalue corresponds to the direction of greatest variance. The corresponding eigenvector is the projection of the PCA-defined AA axis onto the transverse plane. The second eigenvalue and eigenvector represent the PCA-corrected FE axis (Appendix B). The unit length PCA-corrected FE axis lies in the transverse plane with two-dimensional coordinates in the thigh segment coordinate system. In order to conduct the TCPE or PS analyses with PCA-correction, the FE axis must be defined in three dimensions during the static pose configuration in the global coordinate system— i.e. the coordinate system of the gait platform in which all the markers and other vectors are defined. Since the PCA-defined FE axis lies in the transverse plane, the z-component of this vector—the direction of the thigh vector—is equal to zero.

In order to transform the PCA-defined FE axis from the thigh segment coordinate system to the global coordinate system, a transformation matrix, **R**, was derived. The basis vectors of the thigh segment coordinate system can be defined by their coordinates in the global coordinate system (Eqn. 14). Therefore, the transformation from the global to the thigh coordinate system can be defined by setting the rows of the matrix equal to the x-, y-, and z-components of the three coordinate basis vectors.

$$[\boldsymbol{x}_{thigh}] = \begin{bmatrix} x_x \\ y_x \\ z_x \end{bmatrix},\ [\boldsymbol{y}_{thigh}] = \begin{bmatrix} x_y \\ y_y \\ z_y \end{bmatrix},\ [\boldsymbol{z}_{thigh}] = \begin{bmatrix} x_z \\ y_z \\ z_z \end{bmatrix} \tag{14}$$

$$\begin{bmatrix} \boldsymbol{x}_{thigh} \\ \boldsymbol{y}_{thigh} \\ \boldsymbol{z}_{thigh} \end{bmatrix} = \begin{bmatrix} x_x & y_x & z_x \\ x_y & y_y & z_y \\ x_z & y_z & z_z \end{bmatrix} \begin{bmatrix} \boldsymbol{x}_{global} \\ \boldsymbol{y}_{global} \\ \boldsymbol{z}_{global} \end{bmatrix} \tag{15}$$

In order to transform vectors from the thigh coordinate system to the global coordinate system, the vectors must be multiplied by the inverse of the transformation matrix above. The transformation matrix is proper orthogonal, which allows the inverse of the matrix to be calculated from the transpose of the matrix. Therefore, the transformation matrix, **R**, is defined as:

$$\boldsymbol{R} = \begin{bmatrix} x_x & y_x & z_x \\ x_y & y_y & z_y \\ x_z & y_z & z_z \end{bmatrix}^T = \begin{bmatrix} x_x & x_y & x_z \\ y_x & y_y & y_z \\ z_x & z_y & z_z \end{bmatrix} \tag{16}$$

The transformation matrix, **R**, was used to transform the PCA-corrected FE axis to the global coordinate system (Eqn 17).

$$\boldsymbol{FE}_{PCA,global} = \boldsymbol{R}\,\boldsymbol{FE}_{PCA,thigh} \tag{17}$$

The STA analyses were performed using the PCA-corrected FE axis as **I** and the cross product of the thigh vector with the PCA-defined FE axis as **J**. The TCPE method with PCA correction will be referred to as PCA-TCPE angles and the PS method with PCA correction will be referred to as PCA-PS angles.

2.4 Statistics

2.4.1 Triangular Cosserat Point Element (TCPE) Analysis

An initial analysis to test the TCPE method for youth participants was conducted. Since the PS method is the most commonly used bone pose estimator, it was considered the gold standard with which to compare the TCPE method [20]. In order to test that the TCPE method was able to correct for STA in youth participants, it was expected that the uncorrected angles would differ from both the PS angles and TCPE angles, and that the PS and TCPE angles would not statistically differ. In order to test this hypothesis on a participant-specific basis, for each of the six gait trials, the root mean square errors (RMSEs) were calculated for three cases: between the uncorrected and PS knee angles (UC-PS), between the uncorrected and TCPE angles (UC-TCPE), and between the PS and TCPE angles (PS-TCPE). It was hypothesized that, for each participant, the RMSE values would differ and, further, that the RMSE values between PS-TCPE angles would be lower than between UC-TCPE and UC-PS angles. Since there are three cases with repeated measures for each of the six trials, a repeated measures ANOVA was conducted to determine any differences between cases. The RMSE method (UC-TCPE, UC-PS or PS-TCPE) was set as a fixed factor and the trial was set as a random factor. A post-hoc Tukey test was used to distinguish which cases were different.

2.4.2 Principal Component Analysis (PCA)

The goal of PCA is to reduce the correlation between FE-AA angles. This correlation was quantified by conducting a linear regression analysis between the FE and AA angles with AA angles as the dependent variable and finding the R^2 values for the correlations. The linear regression was conducted on all six trials of each participant for the PS, TCPE, PCA-TCPE and PCA-PS angles. It was hypothesized that the R^2 values would differ between the four methods. In order to test this hypothesis, a repeated measures ANOVA was conducted for each participant with the angle calculation method as the fixed factor and the trial as a random factor.

Chapter 3

RESULTS

3.1 Triangular Cosserat Point Element (TCPE) Results

3.1.1 Participant 1

Figure 3.1 shows the FE, AA and IE rotation angles for UC, TCPE and PS methods. Figure 3.2 shows the results of the repeated measures ANOVA of the RMSE values. RMSE values for participant 1 statistically differed between UC-TCPE and PS-TCPE methods and between UC-PS and PC-TCPE for FE, AA, and IE angles ($p<0.001$). RMSE values did not statistically differ between UC-TCPE and UC-PS for FE ($p=0.380$), AA ($p=0.986$) or IE ($p=0.990$) angles. The outputs for all the statistical analyses are shown in Appendix F.

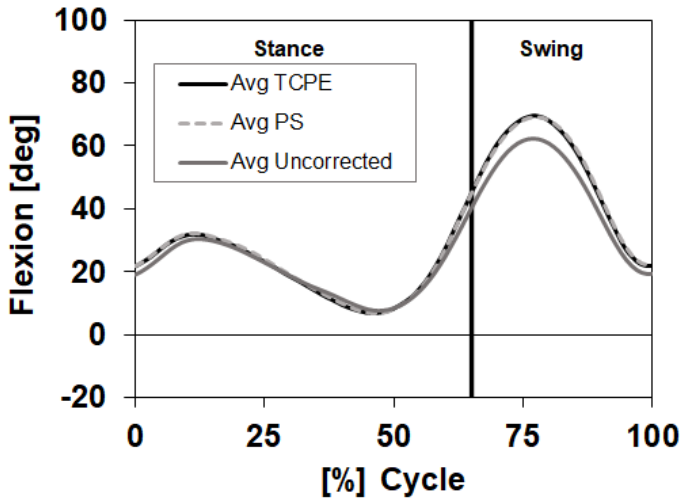

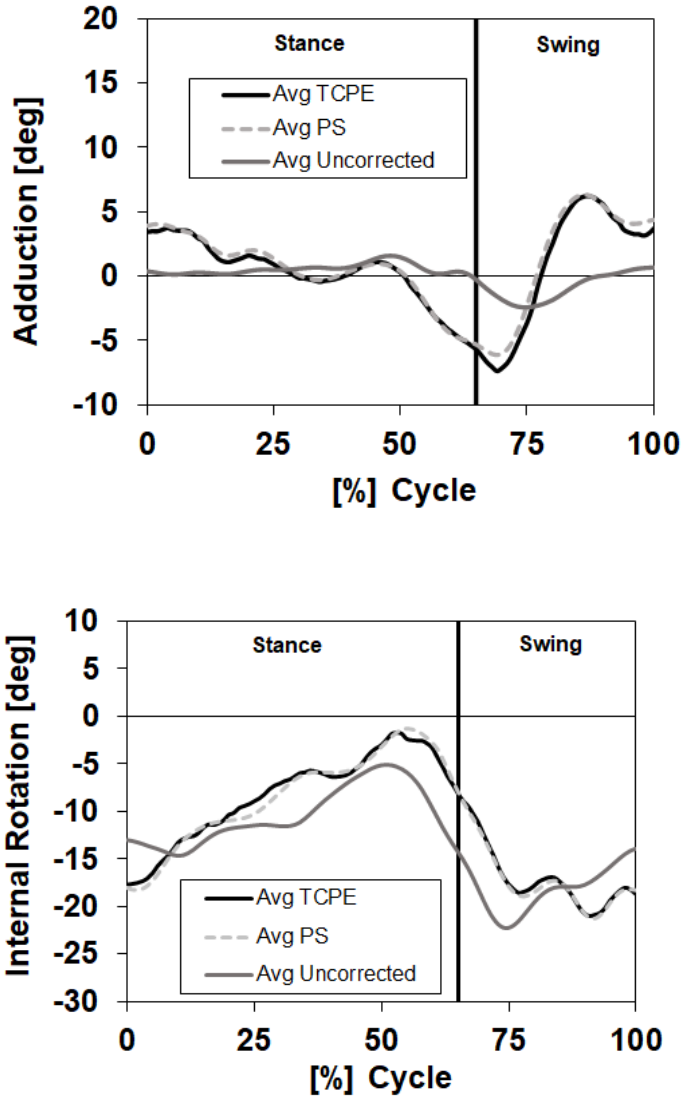

Figure 3.1: Six trial averages of the right knee FE (top), AA (middle), and IE (bottom) angles throughout a gait cycle for Uncorrected, PS and TCPE analysis methods.

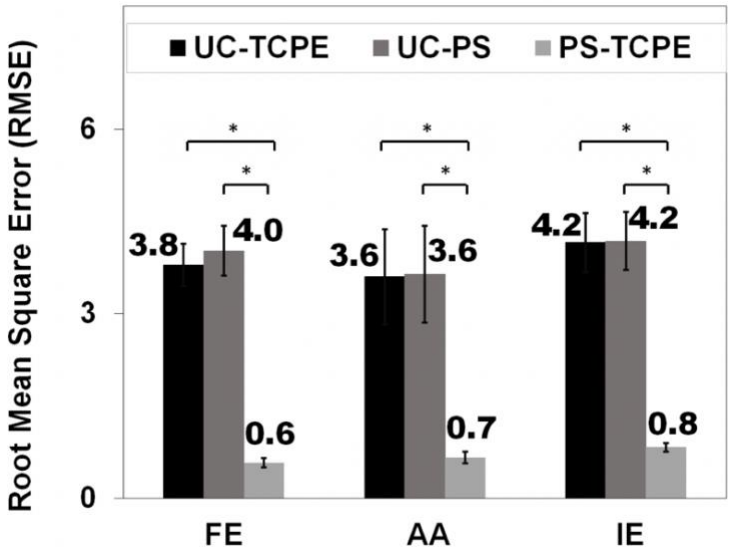

Figure 3.2: RMSE averages between Uncorrected-TCPE, Uncorrected-PS and PS-TCPE methods for FE, AA, and IE angles for participant 1. * indicates statistical significance between groups, p<0.05.

3.1.2 Participant 2

Figure 3.3 shows the FE, AA and IE rotation angles for UC, TCPE and PS methods and Figure 3.4 shows the results of the repeated measures ANOVA of the RMSE values. RMSE values for participant 2 were statistically different between UC-TCPE and PS-TCPE methods and between UC-PS and PS-TCPE for FE, AA and IE angles (p<=0.001). RMSE values did not statistically differ between UC-TCPE and UC-PS for FE (p=0.995), AA (p=0.771) or IE (p=0.745) angles.

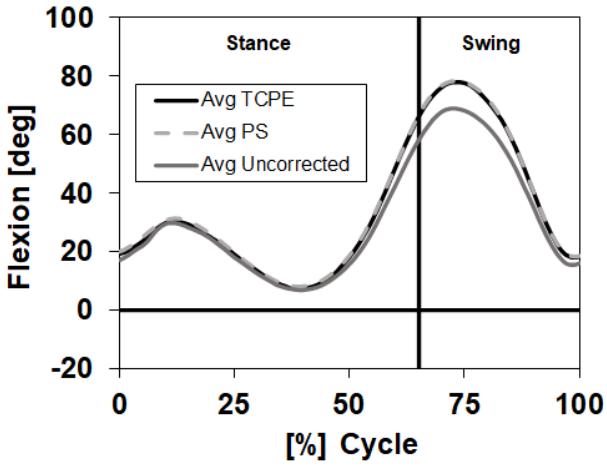

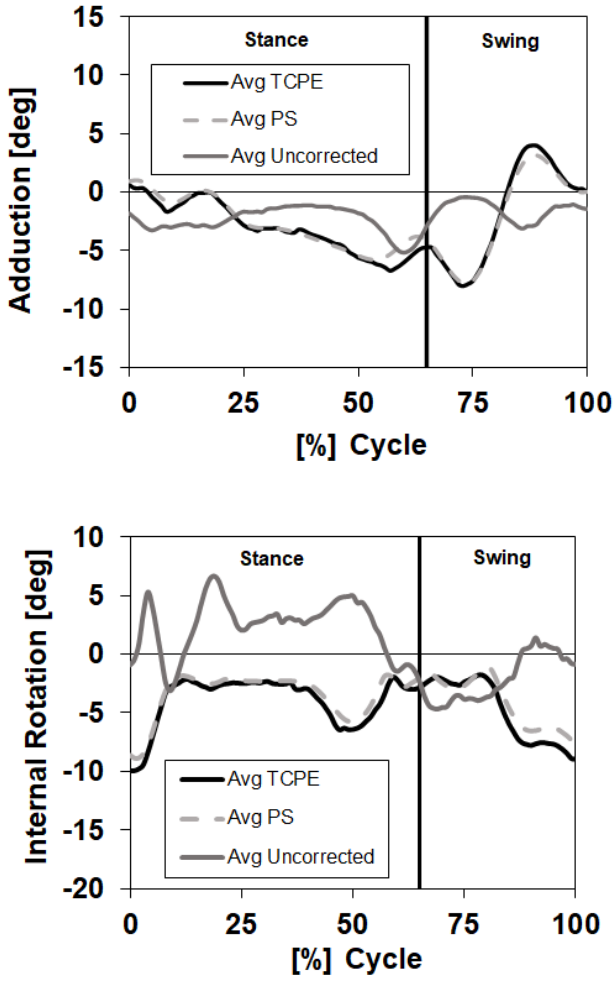

Figure 3.3: Six trial averages of the right knee FE (top), AA (middle), and IE (bottom) angles throughout a gait cycle for Uncorrected, PS and TCPE analysis methods.

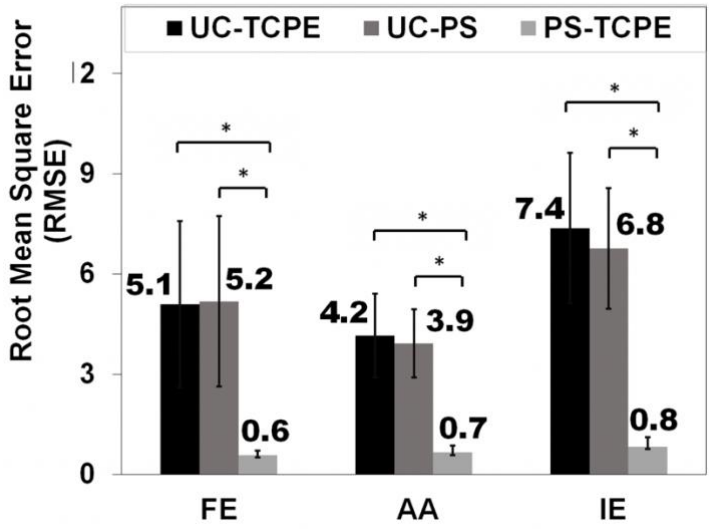

Figure 3.4: RMSE averages between Uncorrected-TCPE, Uncorrected-PS and PS-TCPE methods for FE, AA, and IE angles. * indicates statistical significance between groups, $p<0.05$.

3.2 Principal Component Analysis (PCA) Results

3.2.1 Participant 1

FE, AA, and IE angles are shown in Figure 3.5 for the six-trial averages for pre- and post-PCA correction. The FE angles did not change in a qualitative manner after PCA-correction for TCPE or PS. The AA angles show an upward shift, introducing more adduction, and IE angles show a downward shift, introducing more external rotation, after PCA-correction. The angle plots of the six individual trials are shown in Appendix D.

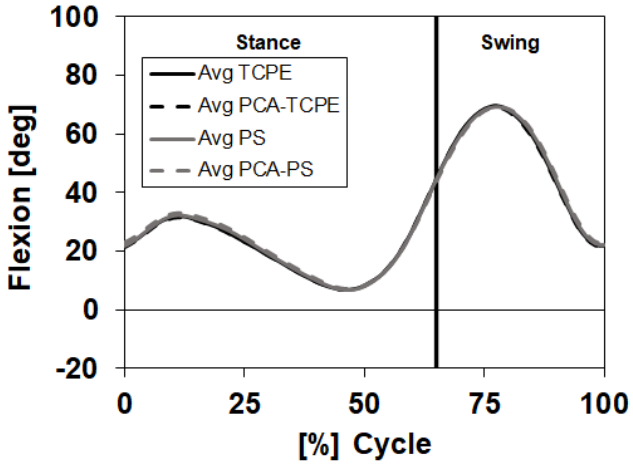

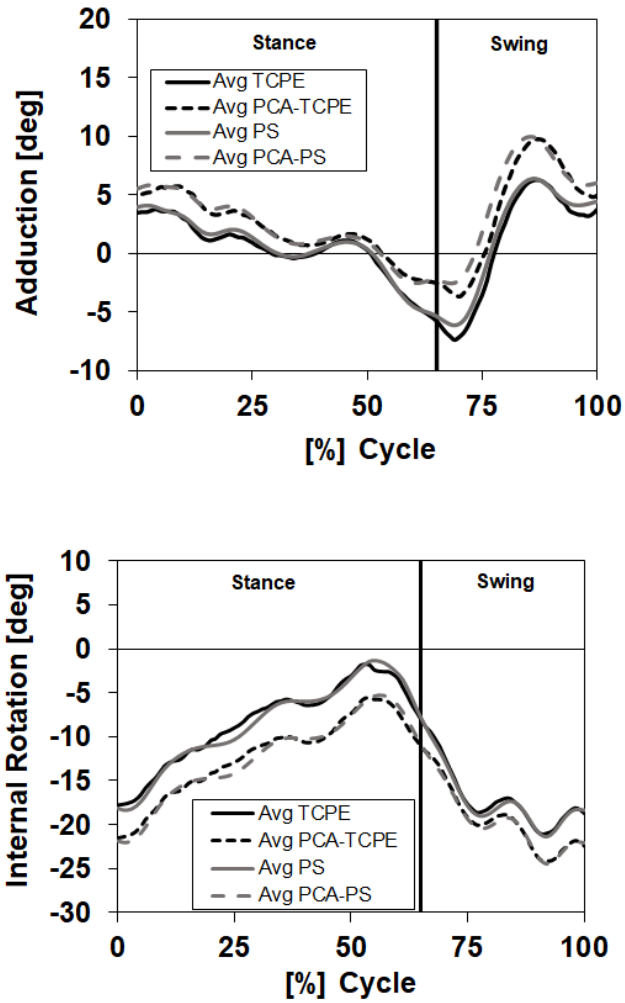

Figure 3.5: Six trial averages for FE (top), AA (middle), and IE (bottom) angles of the TCPE, PS, PCA-TCPE and PCA-PS knee angle results for participant 1.

The linear regression analysis resulted in R^2 correlation values ranging from 0 to 0.2532 and p-values ranging from <0.001 to 0.978 (Table 3.1). The mean R^2 value for each method across all six trials ranged from 0.03 and 0.07. The repeated measures ANOVA yielded a p-value of 0.838, implying that there were not significant differences in the group means of the R^2 values.

Table 3.1: FE-AA linear regression R^2 values and corresponding p-values and repeated measures ANOVA mean R^2 values by method for participant 1. * indicates a statistically significance correlation, p<0.05.

	Method							
	TCPE		**PCA-TCPE**		**PS**		**PCA-PS**	
Trial	R^2	p-value	R^2	p-value	R^2	p-value	R^2	p-value
1	0.0000	0.978	0.0631	0.011*	0.0182	0.180	0.1356	<0.001*
2	0.0221	0.138	0.0359	0.058	0.0028	0.603	0.0747	0.001*
3	0.0017	0.682	0.0107	0.304	0.0082	0.369	0.0535	0.006*
4	0.0113	0.290	0.0146	0.229	0.0021	0.653	0.0307	0.080
5	0.0001	0.931	0.0391	0.047*	0.0018	0.675	0.0653	0.010*
6	0.2532	<0.001*	0.0591	0.014*	0.2038	<0.001*	0.0304	0.810
Mean	0.0481		0.0371		0.0395		0.0650	

The maximum and minimum angles and the angle range for the average AA and IE angles are reported in Table 3.2. The ranges for all methods were between 12.5º and 13.7º for AA angles and between 18.7º and 20.0º for IE angles. The mean AA angles were between 0.5º and 0.9º for TCPE and PS, and between 2.2º and 2.7º for the PCA-corrected methods. The mean IE angles were between -11.3º and -11.6º for TCPE and PS, and between -14.1º and -14.4º for the PCA-corrected methods.

Table 3.2: Maximum, minimum and mean angles and angle range in degrees for average AA and IE angles for participant 1. AA: positive values represent adduction, negative values represent abduction. IE: positive values represent internal rotation, negative values represent external rotation.

		TCPE	PCA-TCPE	PS	PCA-PS
AA	Max	6.277	9.124	6.364	9.320
	Min	-7.344	-4.360	-6.139	-3.181
	Range	13.621	13.484	12.503	12.500
	Mean	0.533	2.267	0.876	2.623
IE	Max	-1.786	-4.815	-1.367	-4.506
	Min	-21.052	-23.577	-21.303	-23.912
	Range	19.266	18.762	19.937	19.406
	Mean	-11.392	-14.129	-11.589	-14.339

3.2.2 Participant 2

The six-trial averages for PCA-corrected FE, AA, and IE angles are compared to pre-correction angles for participant 2 in Figure 3.6. The knee angles calculated with TCPE, PS, PCA-TCPE and PCA-PS methods did not change in a qualitative manner for FE, AA, and IE angles for participant 2. The angle plots for the six individual trials are shown in Appendix D.

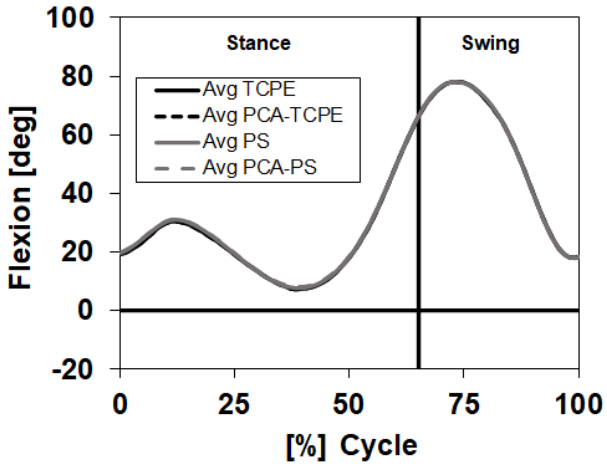

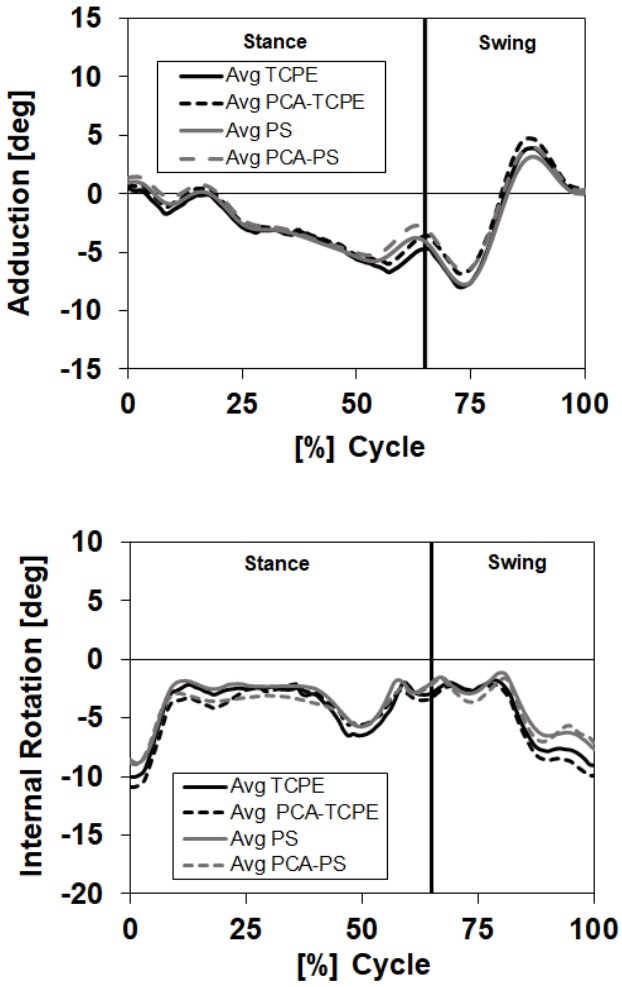

Figure 3.6: Six trial averages for FE (top), AA (middle), and IE (bottom) angles of the TCPE, PS, PCA-TCPE and PCA-PS knee angle results for participant 2.

The linear regression resulted in a range of R^2 values from <0.0001 to 0.2739 and p-values ranging from <0.001 to 0.949 (Table 3.3). Trial 5 exhibited the largest R^2 values before and after PCA-correction, while trial 6 showed a large R^2 value before PCA-correction and decreased after. The p-values of the linear regressions are indicated and the average R^2 value for each method are recorded in Table 3.3. The average R^2 values across all six trials are between 0.04 and 0.09. The repeated measures ANOVA yielded a p-value of 0.838, implying that there were not significant differences in the group means of the R^2 values.

Table 3.3: FE-AA correlation linear regression R^2 values and corresponding p-values and repeated measures ANOVA mean R^2 values by method for participant 2. * indicates a statistically significance correlation, p<0.05.

	TCPE		PCA-TCPE		PS		PCA-PS	
Trial	**R^2**	**p-value**	**R^2**	**p-value**	**R^2**	**p-value**	**R^2**	**p-value**
1	0.0170	0.193	0.0060	0.443	0.0513	0.023*	0.0282	0.093
2	0.0030	0.587	0.0012	0.728	0.0001	0.914	0.0010	0.925
3	0.0157	0.212	0.0002	0.897	0.0132	0.253	<0.0001	0.949
4	0.0122	0.271	0.0085	0.358	0.0157	0.211	0.0076	0.294
5	0.2202	<0.001*	0.2739	<0.001*	0.2025	<0.001*	0.2417	<0.001*
6	0.2179	<0.001*	0.0021	0.649	0.1831	<0.001*	0.0034	0.805
Average	0.0810		0.0454		0.0777		0.0458	

Table 3.4 shows the maximum and minimum angles and the angle ranges for the average AA and IE angle results. The ranges for all four methods are between 10.6º and 12.0º for AA angles and between 7.4º and 8.7º for IE angles. The mean AA angles were between -1.9º and -2.7º for all methods. The mean IE angles were between -3.6º and -4.7º for all methods.

Table 3.4: Maximum, minimum and mean angles and angle range in degrees for average AA and IE angles for participant 2. AA: positive values represent adduction, negative values represent abduction. IE: positive values represent internal rotation, negative values represent external rotation

		TCPE	PCA-TCPE	PS	PCA-PS
AA	Max	3.942	4.539	3.182	3.775
	Min	-8.027	-7.125	-7.777	-6.877
	Range	11.969	11.665	10.960	10.652
	Mean	-2.620	-2.168	-2.447	-1.987
IE	Max	-1.821	-2.187	-1.081	-1.521
	Min	-9.973	-10.833	-8.839	-8.936
	Range	8.152	8.647	7.758	7.415
	Mean	-4.315	-4.664	-3.623	-4.087

Chapter 4
DISCUSSION

The pilot gait experiments with youth participants proved to be successful overall for data collection with small modifications in the experimental procedure used for adult participants. The adjustment of the gait platform to decrease the distance between force plates for the shorter stride length of children was sufficient for both participants to make foot contact with every force plate without noticeable changes in their natural gait. The use of seven markers for the TCPE clusters on the thigh and shank segments was a concern due to the smaller leg size of children. However, the use of the seven-marker clusters was successful and did not yield marker confusion during recording which can occur when there is not adequate distance between markers.

The TCPE method of STA correction yielded knee angles following trends typical for FE, AA, and IE angles for both participants. The repeated measures ANOVA concluded that the TCPE and PS methods yielded different results than the UC angles, but the results did not differ between the TCPE and PS method angles. This suggests that either method is sufficient for STA correction and will yield similar knee angle results. One benefit of using the TCPE method is the separation of STA due to strain, relative translation and relative rotation modes. In this analysis, the three categories of STA were evenly weighted in the filtering criteria for TCPE selection, which yielded similar rotation tensors as those calculated by the PS method. Further research with the TCPE method could examine the results with variations in the weighting of the categories to test whether that may improve the knee angle calculations with skin markers.

The FE-AA correlation results from the linear regression analyses are detailed in Tables 3.1 and 3.3. Some of the p-values are less than 0.05, indicating a statistically significant correlation between the FE and AA angles. However, the coefficients of the linear regressions are very small—all less than 0.08—which implies that the correlations between the angles, while significant, are not suggestive of considerable crosstalk.

The statistical analyses for PCA-corrected knee angles did not yield statistical differences between any of the four method groups, indicating that there were not significant decreases in the FE-AA correlations for either participant. There are a few potential causes for the lack of improvement in correlations after PCA-correction. Firstly, the correlations seen with STA

correction are far less linear than the correlations before STA correction (Appendix E). The trends seen in the uncorrected angle correlations are more typical to FE-AA correlation plots, while the STA-corrected FE-AA correlations show changes to the linearity of the data. A potential explanation for these unexpected correlations may be due to STA introducing errors in the AA angles and producing non-physiological FE-AA correlations. STA-correction methods may reduce these errors but not completely eliminate them. It is thought that, without correction methods, the movement of the skin markers may mask the true movement of the underlying bone segment [19]. Additionally, it has been shown that STA can result in misleading angle patterns for AA and IE [16]. STA correction methods aim to find the best predictors for the underlying bone segment in order to compute knee angles. However, if STA is large for all datapoints, even the best predictors may still retain errors from STA which carry over into the results. It has been shown that errors from STA tend be substantially greater during the swing phase than the stance phase [22]. The FE-AA correlation results during swing versus stance phase can be seen in Appendix E. Future studies comparing the correlations after STA correction should separate the results between the swing and stance phases to determine whether there are differences in the trends seen in the correlations between the phases. Additionally, the FE-AA correlations should be examined in previous adult gait studies with STA correction to compare patterns and results to those seen for the youth participants in this study.

Another potential reason that the correlations did not improve after STA correction could be that the marker placement was accurate enough to not experience large correlations before the PCA analysis due to placement by a trained professional. Therefore, there would not be much crosstalk for PCA to correct or for the results to show a significant difference. The substantial correlation changes after PCA-correction are often calculated with purposely and drastically misplaced markers to represent the worse possible scenario of misplacement [18]. However, this study only included one marker placement for each participant with the most accurate placement possible. Additionally, most previous studies examining crosstalk were conducted with adult participants. It is possible that crosstalk is less of a concern with youth participants due to differences such as easier location of key anatomical positions or a lesser amount of soft tissue.

Tables 3.2 and 3.4 describe the maximum, minimum, mean and range of the angles for participants 1 and 2, respectively. The range of the angles remains relatively constant, while the maximum and minimum values change. This implies that the PCA analysis is not decreasing the FE-AA correlation, since a decrease in correlation is caused mostly by a decrease in the range of the AA angles. The changes in the maximum and minimum values of the plots indicate that the range was similar but there was an offset in the FE and AA angles. For participant 1, the mean AA angles show an offset of approximately 2°, introducing more adduction, and the mean IE angles show an offset of almost -3°, introducing more external rotation after PCA-correction. The mean angles for participant 2 had smaller offsets, with an AA angle offset of about 0.5° and an IE angle offset of almost 0.4°. These offsets caused by the PCA analysis are due to the new definition of the FE axis having greater angles of adduction and external rotation in the static configuration. In order to further analyze this discrepancy, the angles between the marker-based and the PCA-corrected FE axes were inspected. The angles between the axes before and after PCA-correction are outlined in Appendix C. For participant 1, the angles were between 3.4° to 5.0° for all trials. However, participant 2 had lower angles, between 0.5 and 1.5° for the first five trials and an angle of 4.7° for the sixth trial. The greater change in the flexion axis for participant 1 explains the offset in the average AA and IE axes. The minimal change of the FE axis for participant 2 confirmed the lower offsets for the AA and IE mean angles.

Differences in the R^2 values of trial 6 for participant 1 and trials 5 and 6 of participant 2 versus previous trials can be seen in Tables 3.1 and 3.3. The correlations seen for these trials are much larger than previous trials for the TCPE and PS methods. Given that these trials were the last to be conducted, the greater correlations may have been cause by accidental movement or adjustment of the markers towards the end of the experiments. The correlations for trial 5 of participant 2 after PCA-correction only slightly differed. However, for trial 6 of each participant, the R^2 values decreased greatly which may indicate that the PCA-correction method does decrease the FE-AA angles correlation when there is inaccurate marker placement.

A limitation of this study was that the data were limited to two participants, which prevented significant statistical conclusions from being made for a population (i.e. children). This

study was intended to have a sufficient number of participants to conduct statistics with a sample group. However, following the experiments with participants 1 and 2, in-person research was halted due to COVID-19 restrictions. The statistical analyses conducted within this study were all performed in a participant specific manner to examine the results of the methods. However, these results should not be assumed to apply to the youth population as it is not statistically valid to do so.

This study suggests that similar experimental methods and post-hoc correction methods that are currently used for adult gait knee kinematics analyses can be applied to youth participants with minor modifications in the experimental data collection procedure. These methods can be used to conduct minimally invasive studies with children to gain knowledge regarding the normal knee kinematics in youth during gait. Future work should include a larger sample size of youth participants and include various weight categories, such as normal weight, overweight, and obese groups, with which to compare knee kinematic results during gait. Changes in knee kinematics may put certain groups at a higher risk for issues such as osteoarthritis. Understanding potential changes in gait patterns based on weight category would allow for intervention methods, such as diet and exercise, to be developed and implemented to mitigate the risks associated with abnormal gait patterns.

REFERENCES

[1] M. A. Lafortune, P. R. Cavanagh, H. J. Sommer, and A. Kalenak, “Three-dimensional kinematics of the human knee during walking,” *J. Biomech.*, vol. 25, no. 4, 1992, doi: 10.1016/0021-9290(92)90254-X.

[2] P. P. K. Lai, A. K. L. Leung, A. N. M. Li, and M. Zhang, “Three-dimensional gait analysis of obese adults,” *Clin. Biomech.*, vol. 23, no. SUPLL.1, 2008, doi: 10.1016/j.clinbiomech.2008.02.004.

[3] E. Y. Chao, R. K. Laughman, E. Schneider, and R. N. Stauffer, “Normative data of knee joint motion and ground reaction forces in adult level walking,” *J. Biomech.*, vol. 16, no. 3, 1983, doi: 10.1016/0021-9290(83)90129-X.

[4] V. Cimolin and M. Galli, “Summary measures for clinical gait analysis: A literature review,” *Gait and Posture*, vol. 39, no. 4. 2014, doi: 10.1016/j.gaitpost.2014.02.001.

[5] J. Clément, P. Toliopoulos, N. Hagemeister, F. Desmeules, A. Fuentes, and P. A. Vendittoli, “Healthy 3D knee kinematics during gait: Differences between women and men, and correlation with x-ray alignment,” *Gait Posture*, vol. 64, 2018, doi: 10.1016/j.gaitpost.2018.06.024.

[6] P. J. Rowe, C. M. Myles, C. Walker, and R. Nutton, “Knee joint kinematics in gait and other functional activities measured using flexible electrogoniometry: How much knee motion is sufficient for normal daily life?,” *Gait Posture*, vol. 12, no. 2, 2000, doi: 10.1016/S0966-6362(00)00060-6.

[7] K. J. Deluzio, U. P. Wyss, B. Zee, P. A. Costigan, and C. Sorbie, “Principal component models of knee kinematics and kinetics: Normal vs. pathological gait patterns,” *Hum. Mov. Sci.*, vol. 16, no. 2–3, 1997, doi: 10.1016/S0167-9457(96)00051-6.

[8] J. S. Li, T. Y. Tsai, D. T. Felson, G. Li, and C. L. Lewis, “Six degree-of-freedom knee joint kinematics in obese individuals with knee pain during gait,” *PLoS One*, vol. 12, no. 3, 2017, doi: 10.1371/journal.pone.0174663.

[9] R. E. Hutchison, E. M. Lucas, J. Marro, T. Gambon, K. N. Bruneau, and J. D. DesJardins, “The effects of simulated knee arthrodesis on gait kinematics and kinetics,” *Proc. Inst. Mech. Eng. Part H J. Eng. Med.*, vol. 233, no. 7, 2019, doi: 10.1177/0954411919850028.

[10] Y. Nagano *et al.*, “Association between in vivo knee kinematics during gait and the severity of knee osteoarthritis,” *Knee*, vol. 19, no. 5, 2012, doi: 10.1016/j.knee.2011.11.002.

[11] T. P. Andriacchi and A. Mündermann, “The role of ambulatory mechanics in the initiation and progression of knee osteoarthritis,” *Current Opinion in Rheumatology*, vol. 18, no. 5. 2006, doi: 10.1097/01.bor.0000240365.16842.4e.

[12] D. G. Eckhoff, “Effect of limb malrotation on malalignment and osteoarthritis,” *Orthopedic Clinics of North America*, vol. 25, no. 3. 1994, doi: 10.1016/s0030-5898(20)31925-8.

[13] B. Yu, M. J. Stuart, T. Kienbacher, E. S. Growney, and K. N. An, “Valgus-varus motion of the knee in normal level walking and stair climbing,” *Clin. Biomech.*, vol. 12, no. 5, 1997, doi: 10.1016/S0268-0033(97)00005-3.

[14] B. Shabani, D. Bytyqi, S. Lustig, L. Cheze, C. Bytyqi, and P. Neyret, “Gait knee kinematics after ACL reconstruction: 3D assessment,” *Int. Orthop.*, vol. 39, no. 6, 2015, doi: 10.1007/s00264-014-2643-0.

[15] E. Szczerbik and M. Kalinowska, “The influence of knee marker placement error on evaluation of gait kinematic parameters,” *Acta Bioeng. Biomech.*, vol. 13, no. 3, 2011.

[16] M. Akbarshahi, A. G. Schache, J. W. Fernandez, R. Baker, S. Banks, and M. G. Pandy,

"Non-invasive assessment of soft-tissue artifact and its effect on knee joint kinematics during functional activity," *J. Biomech.*, vol. 43, no. 7, 2010, doi: 10.1016/j.jbiomech.2010.01.002.

[17] A. Cappozzo, F. Catani, A. Leardini, M. G. Benedetti, and U. Della Croce, "Position and orientation in space of bones during movement: Experimental artefacts," *Clin. Biomech.*, vol. 11, no. 2, 1996, doi: 10.1016/0268-0033(95)00046-1.

[18] E. Jensen, V. Lugade, J. Crenshaw, E. Miller, and K. Kaufman, "A principal component analysis approach to correcting the knee flexion axis during gait," *J. Biomech.*, vol. 49, no. 9, 2016, doi: 10.1016/j.jbiomech.2016.03.046.

[19] D. L. Benoit, D. K. Ramsey, M. Lamontagne, L. Xu, P. Wretenberg, and P. Renström, "Effect of skin movement artifact on knee kinematics during gait and cutting motions measured in vivo," *Gait Posture*, vol. 24, no. 2, 2006, doi: 10.1016/j.gaitpost.2005.04.012.

[20] V. Camomilla, T. Bonci, R. Dumas, L. Chèze, and A. Cappozzo, "A model of the soft tissue artefact rigid component," *J. Biomech.*, vol. 48, no. 10, 2015, doi: 10.1016/j.jbiomech.2015.05.007.

[21] D. Solav, M. B. Rubin, and A. Wolf, "Soft Tissue Artifact compensation using Triangular Cosserat Point Elements (TCPEs)," *Int. J. Eng. Sci.*, vol. 85, 2014, doi: 10.1016/j.ijengsci.2014.07.001.

[22] D. Solav, V. Camomilla, A. Cereatti, A. Barré, K. Aminian, and A. Wolf, "Bone orientation and position estimation errors using Cosserat point elements and least squares methods: Application to gait," *J. Biomech.*, vol. 62, 2017, doi: 10.1016/j.jbiomech.2017.01.026.

[23] T. P. Andriacchi, E. J. Alexander, M. K. Toney, C. Dyrby, and J. Sum, "A point cluster method for in vivo motion analysis: Applied to a study of knee kinematics," *J. Biomech. Eng.*, vol. 120, no. 6, 1998, doi: 10.1115/1.2834888.

[24] A. Baudet *et al.*, "Cross-talk correction method for knee kinematics in gait analysis using Principal Component Analysis (PCA): A new proposal," *PLoS One*, vol. 9, no. 7, 2014, doi: 10.1371/journal.pone.0102098.

[25] C. Goodall, "Procrustes Methods in the Statistical Analysis of Shape," *J. R. Stat. Soc. Ser. B*, vol. 53, no. 2, 1991, doi: 10.1111/j.2517-6161.1991.tb01825.x.

[26] K. Dudum, "'Placing markers in accordance with enhanced helen hayes.,'" 2015.

[27] S. L. Tucker, S. Weinhardt, C. R. O'Hara, S. J. Hazelwood, and S. M. Klisch, "Knee kinematics for the contralateral knee of transtibial amputees in gait and cycling," *Southwest Am. Coll. Sport. Med. Reg. Chapter Annu. Meet.*, 2019.

[28] J. E. Deschamps and S. M. Klisch, "Pseudo-Rigid Body Method for Reducing Soft Tissue Artifact: Three-Dimensional Validation and Application to Gait."

[29] E. S. Grood and W. J. Suntay, "A joint coordinate system for the clinical description of three-dimensional motions: Application to the knee," *J. Biomech. Eng.*, vol. 105, no. 2, 1983, doi: 10.1115/1.3138397.

APPENDIX A: MATLAB Plots of Lateral Ankle Marker Projections

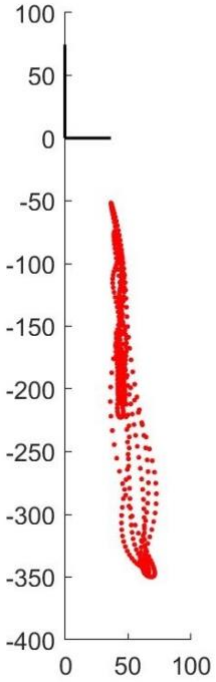

Figure A1: Participant 1 Trial 1

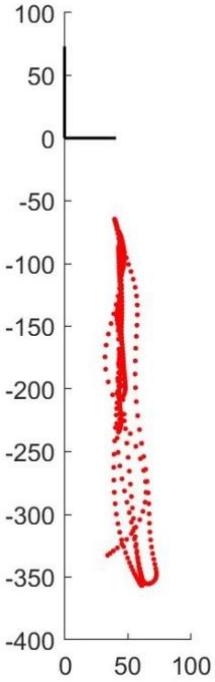

Figure A2: Participant 1 Trial 2

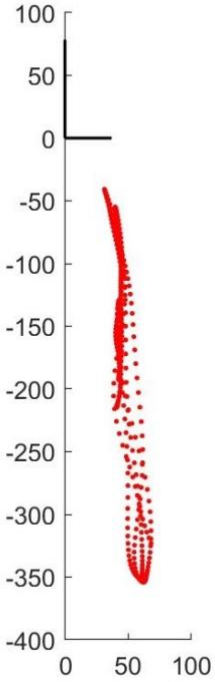

Figure A3: Participant 1 Trial 3

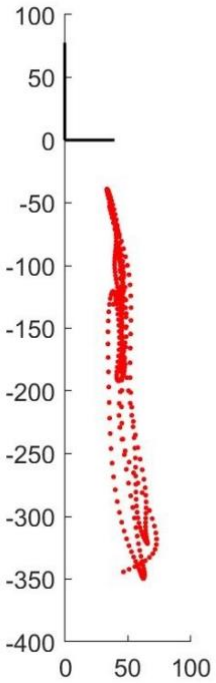

Figure A4 Participant 1 Trial 4

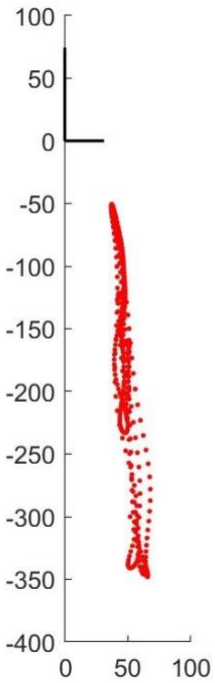

Figure A5: Participant 1 Trial 5

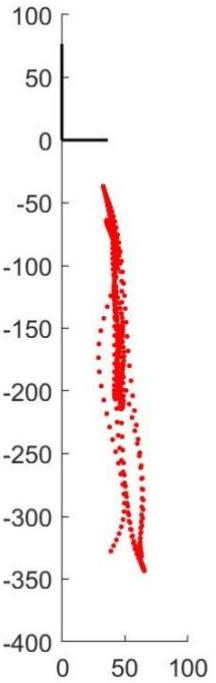

Figure A6: Participant 1 Trial 6

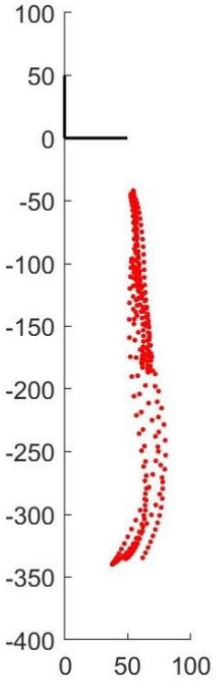

Figure A7: Participant 2 Trial 1

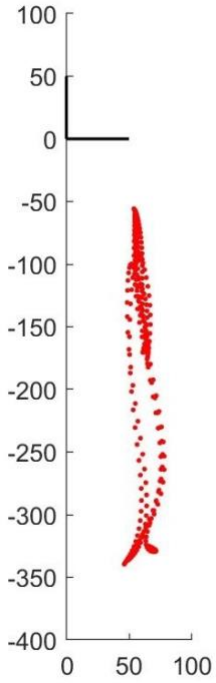

Figure A8: Participant 2 Trial 2

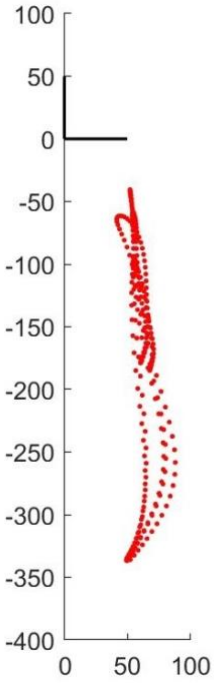

Figure A9: Participant 2 Trial 3

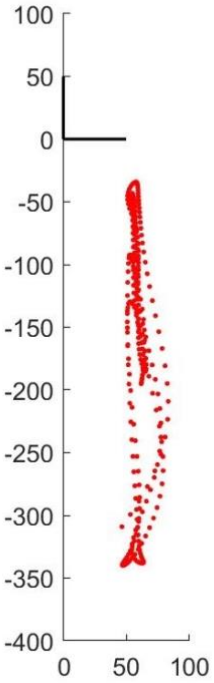

Figure A10: Participant 2 Trial 4

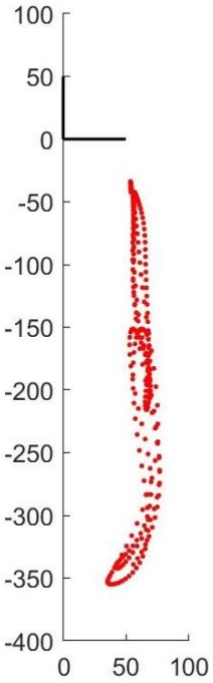

Figure A11: Participant 2 Trial 5

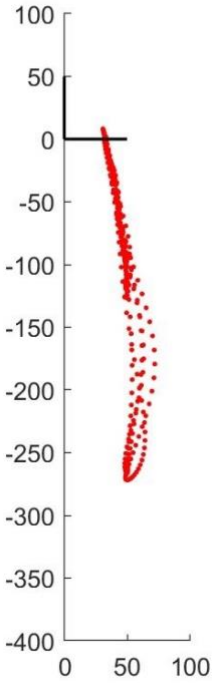

Figure A12: Participant 2 Trial 6

APPENDIX B: PCA Eigenvectors Plots

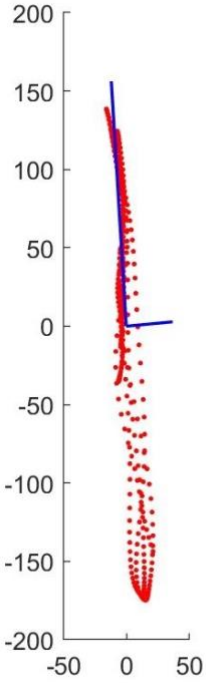

Figure B1: Participant 1 Trial 1

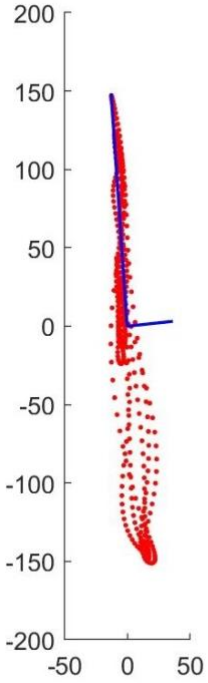

Figure B2: Participant 1 Trial 2

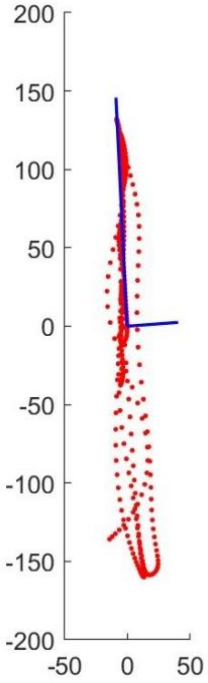

Figure B3: Participant 1 Trial 3

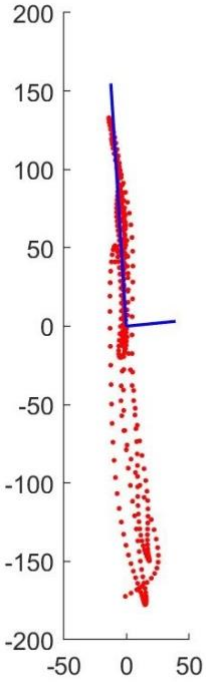

Figure B4 Participant 1 Trial 4

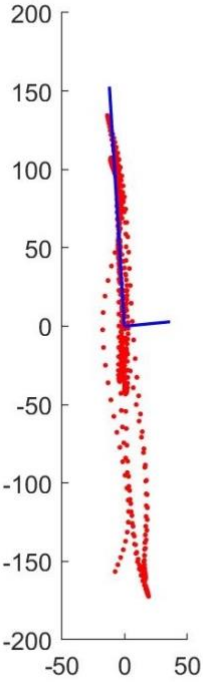

Figure B5: Participant 1 Trial 5

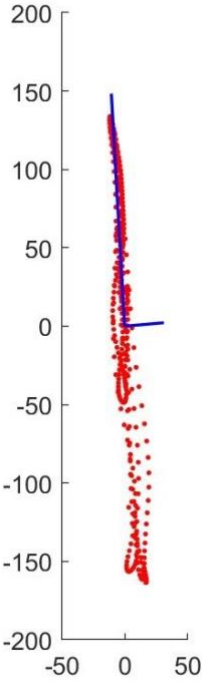

Figure B6: Participant 1 Trial 6

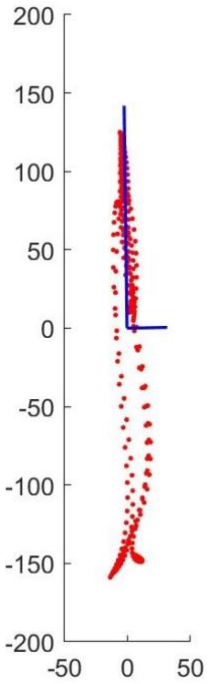

Figure B7: Participant 2 Trial 1

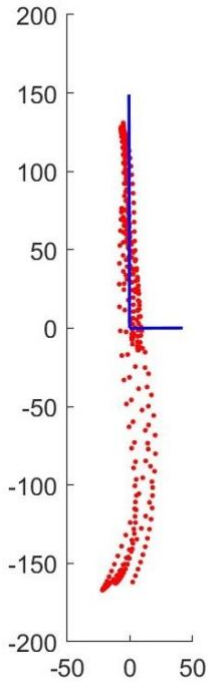

Figure B8: Participant 2 Trial 2

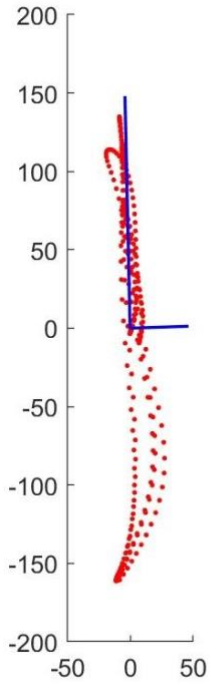

Figure B9: Participant 2 Trial 3

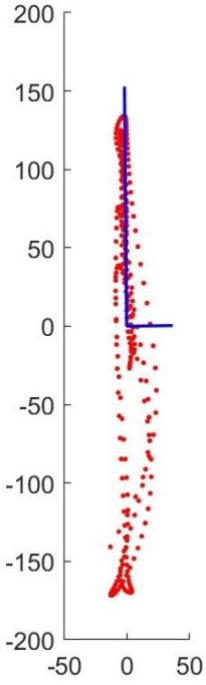

Figure B10: Participant 2 Trial 4

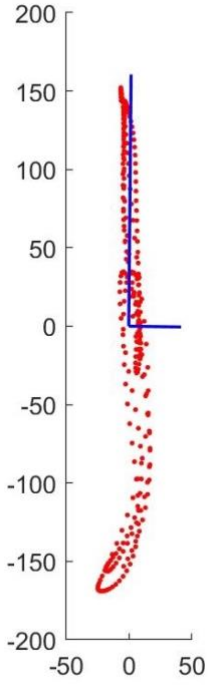

Figure B11: Participant 2 Trial 5

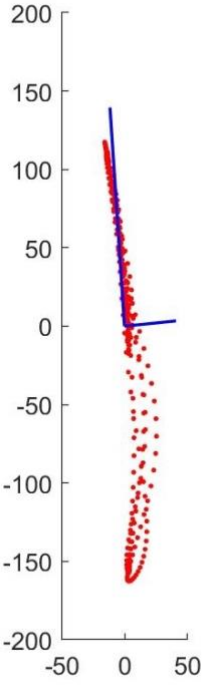

Figure B12: Participant 2 Trial 6

APPENDIX C: Angles Between Marker-Based and PCA-Corrected FE Axes

Table C1: Angle in Degrees between Marker-Based and PCA-Corrected FE Axes

	Trial					
Participant	**1**	**2**	**3**	**4**	**5**	**6**
1	4.3544˚	4.9239˚	3.4623˚	4.4362˚	4.5261˚	4.0630˚
2	0.9307˚	0.1903˚	1.5761˚	0.6580˚	0.6605˚	4.7319˚

APPENDIX D: Individual Trial FE, AA and IE Angle Plots for PCA Analysis

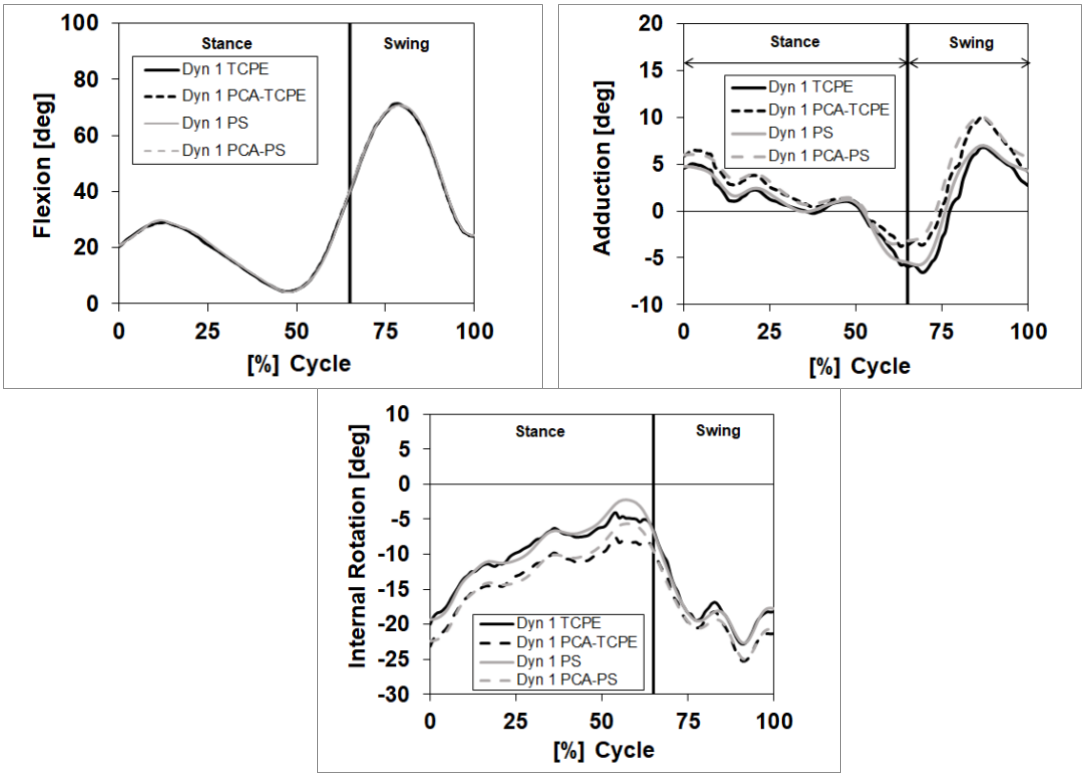

Figure D1: Trial 1 FE (top left), AA (top right) and IE (bottom) angles for participant 1.

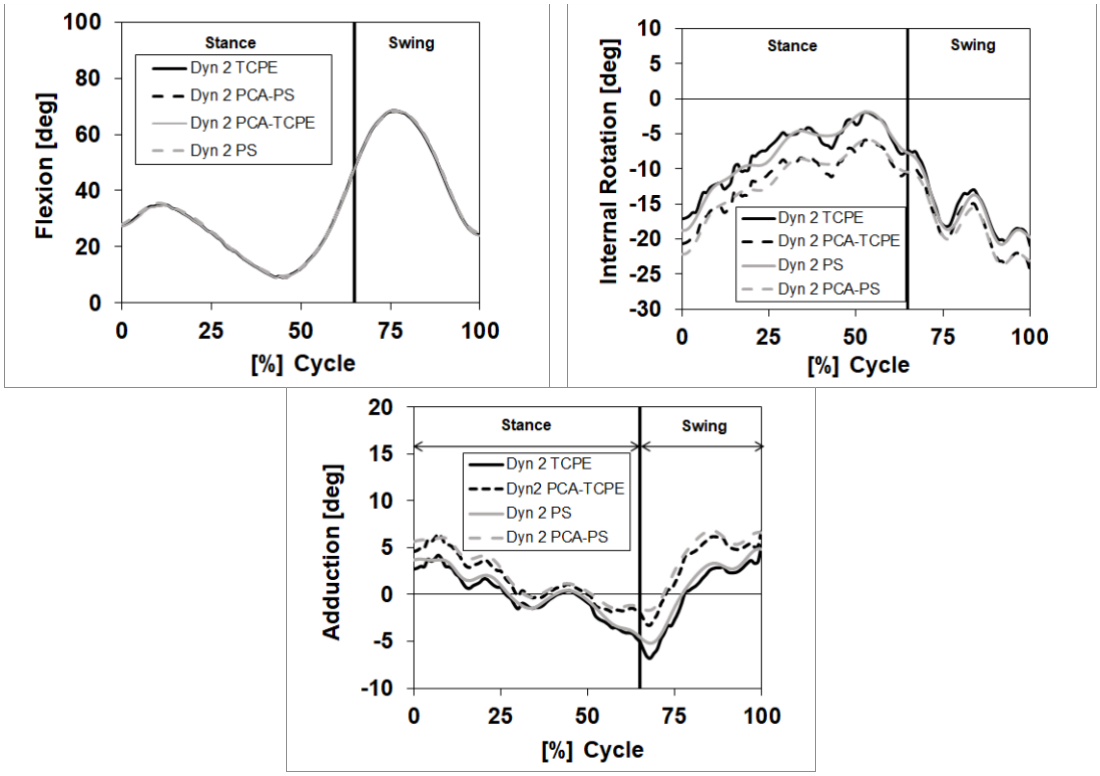

Figure D2: Trial 2 FE (top left), AA (top right) and IE (bottom) angles for participant 1.

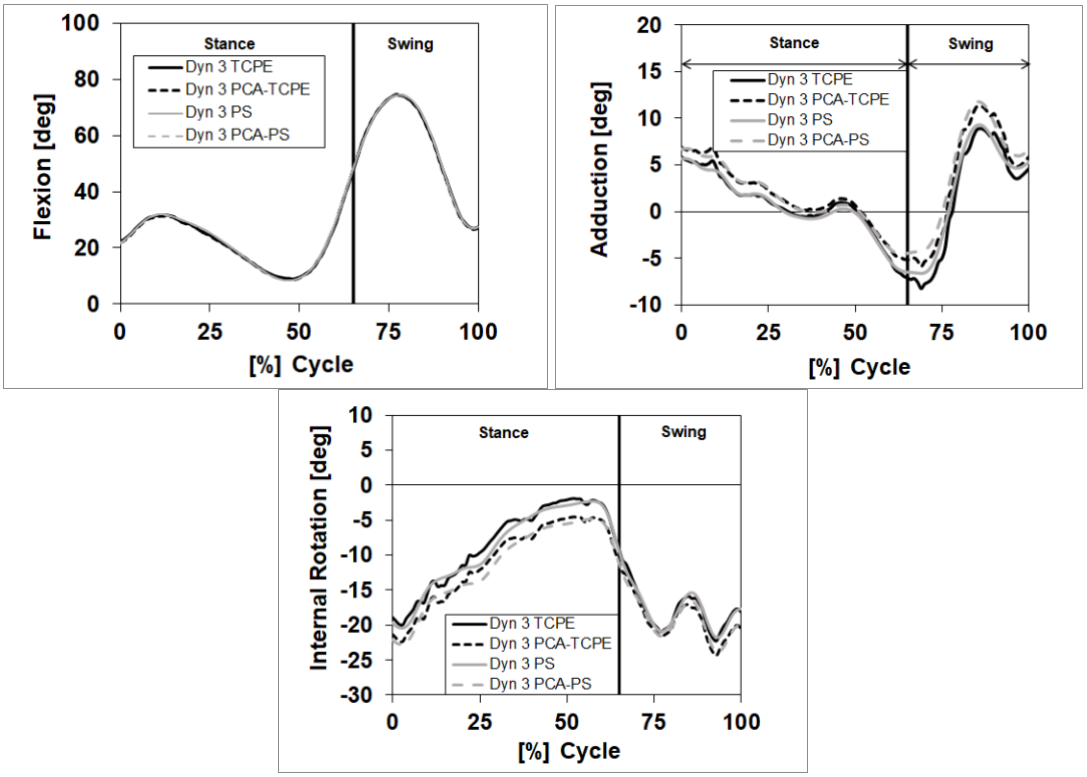

Figure D3: Trial 3 FE (top left), AA (top right) and IE (bottom) angles for participant 1.

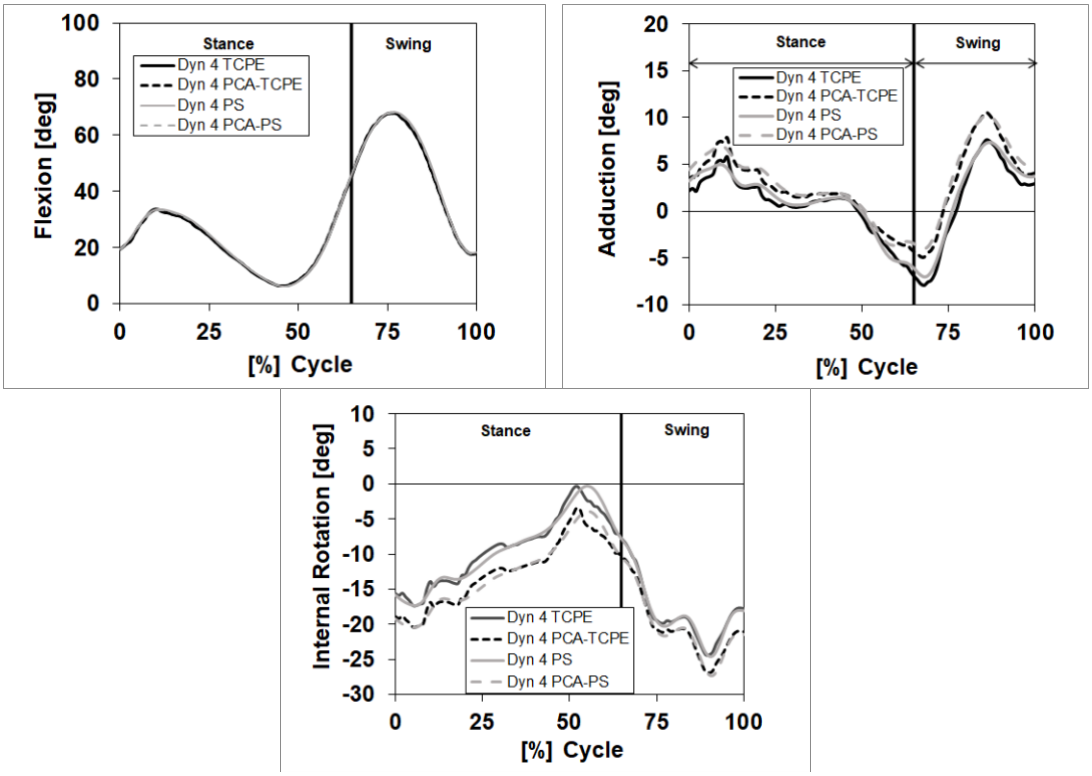

Figure D4: Trial 4 FE (top left), AA (top right) and IE (bottom) angles for participant 1.

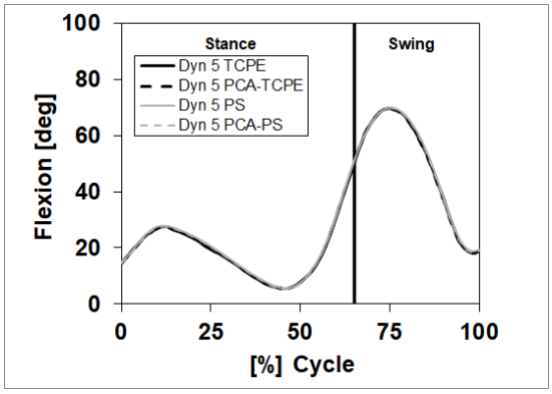

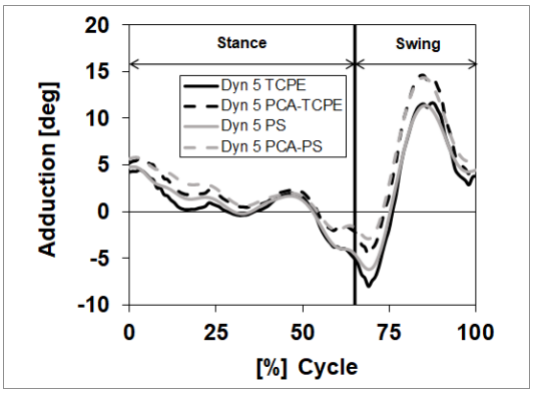

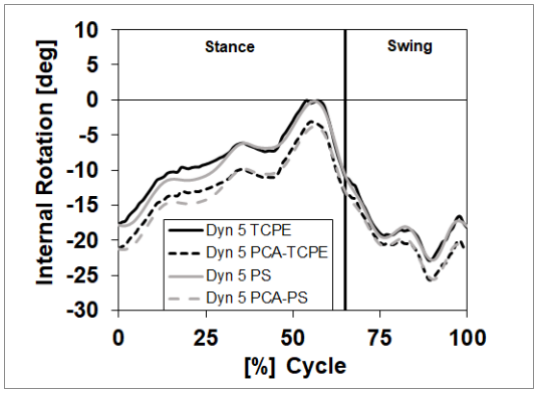

Figure D5: Trial 5 FE (top left), AA (top right) and IE (bottom) angles for participant 1.

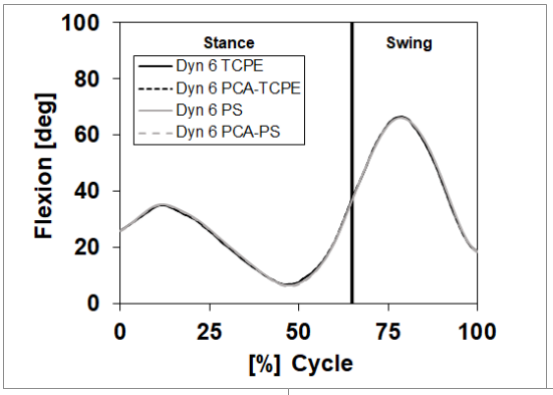

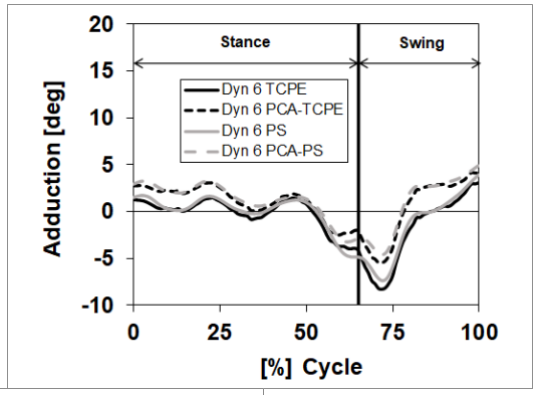

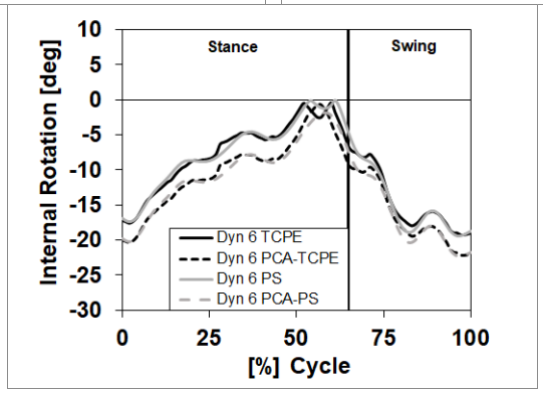

Figure D6: Trial 6 FE (top left), AA (top right) and IE (bottom) angles for participant 1.

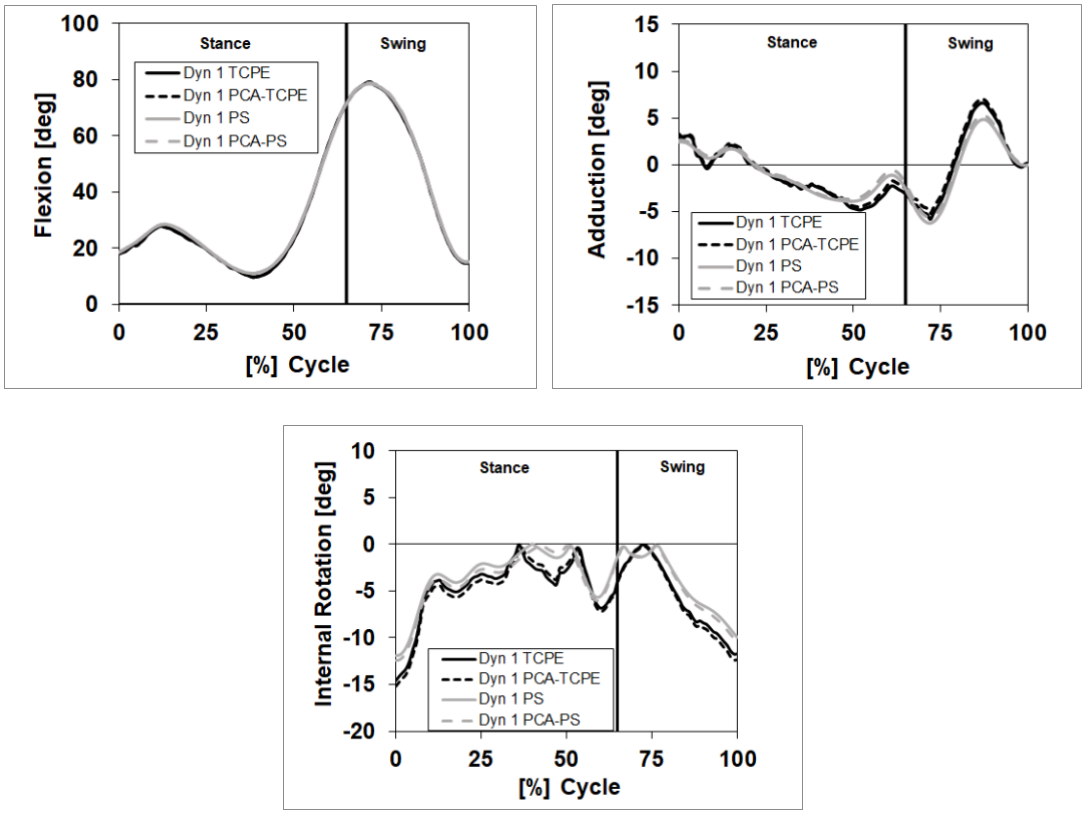

Figure D7: Trial 1 FE (top left), AA (top right) and IE (bottom) angles for participant 2.

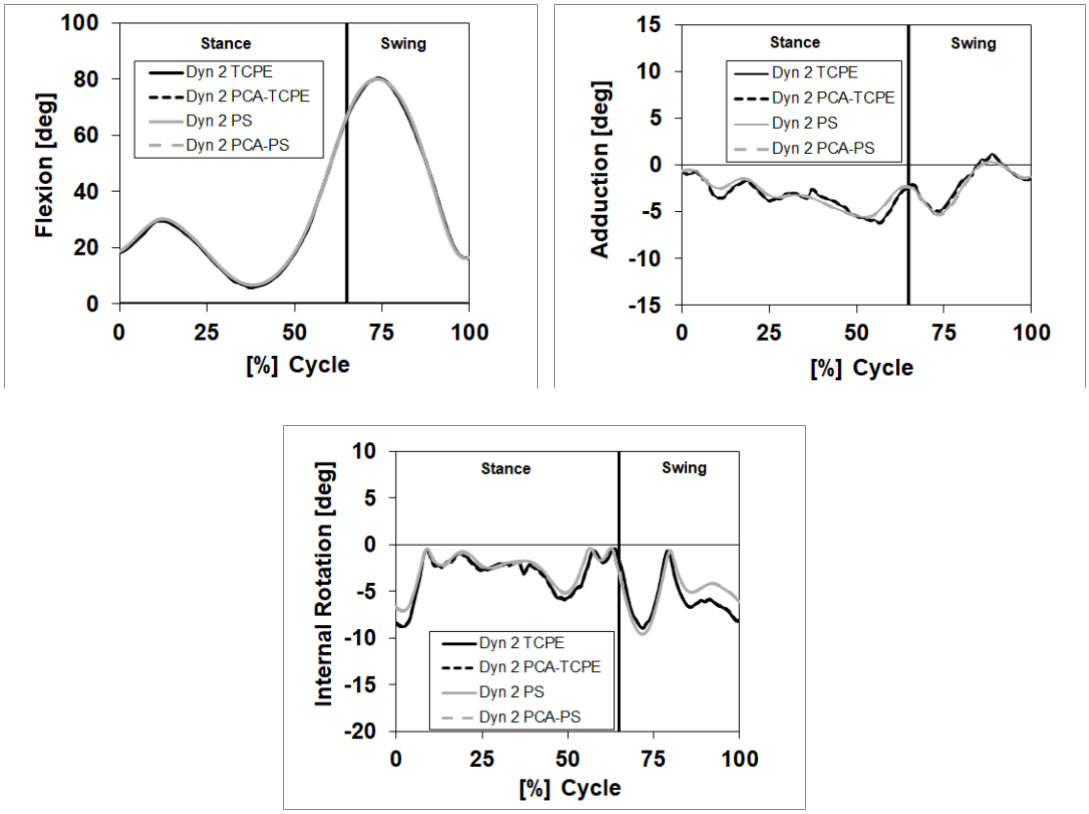

Figure D8: Trial 2 FE (top left), AA (top right) and IE (bottom) angles for participant 2.

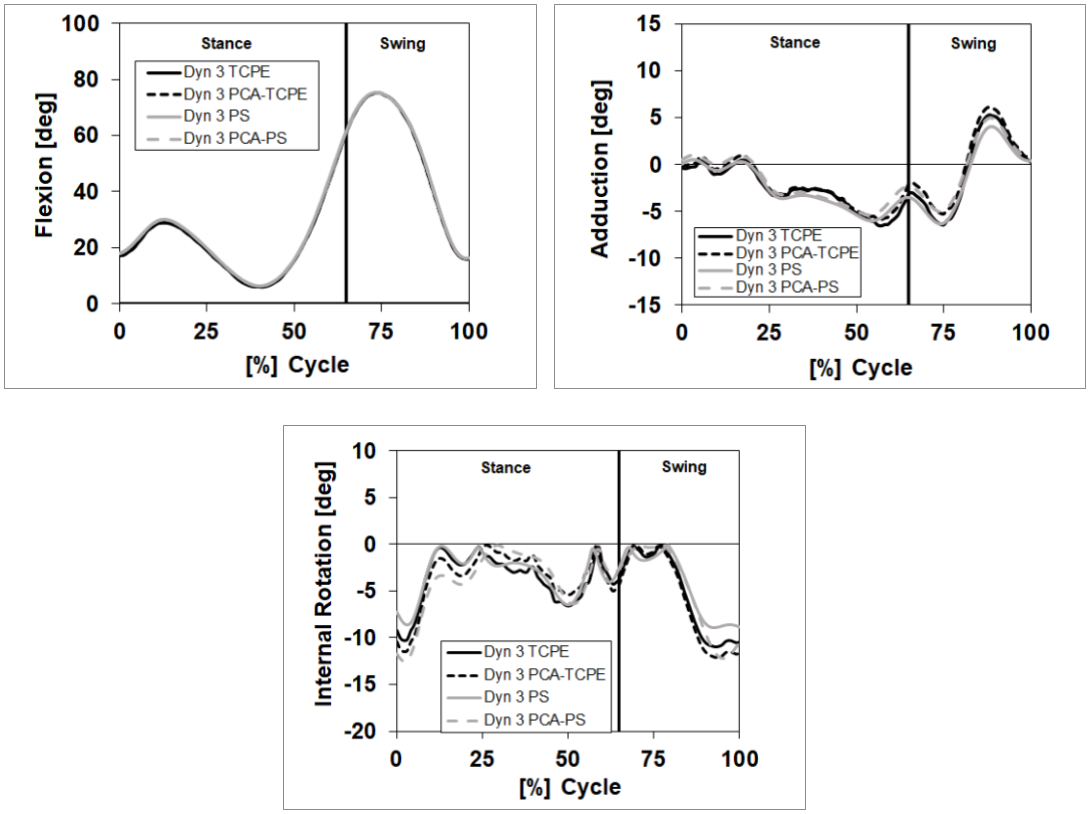

Figure D9: Trial 3 FE (top left), AA (top right) and IE (bottom) angles for participant 2.

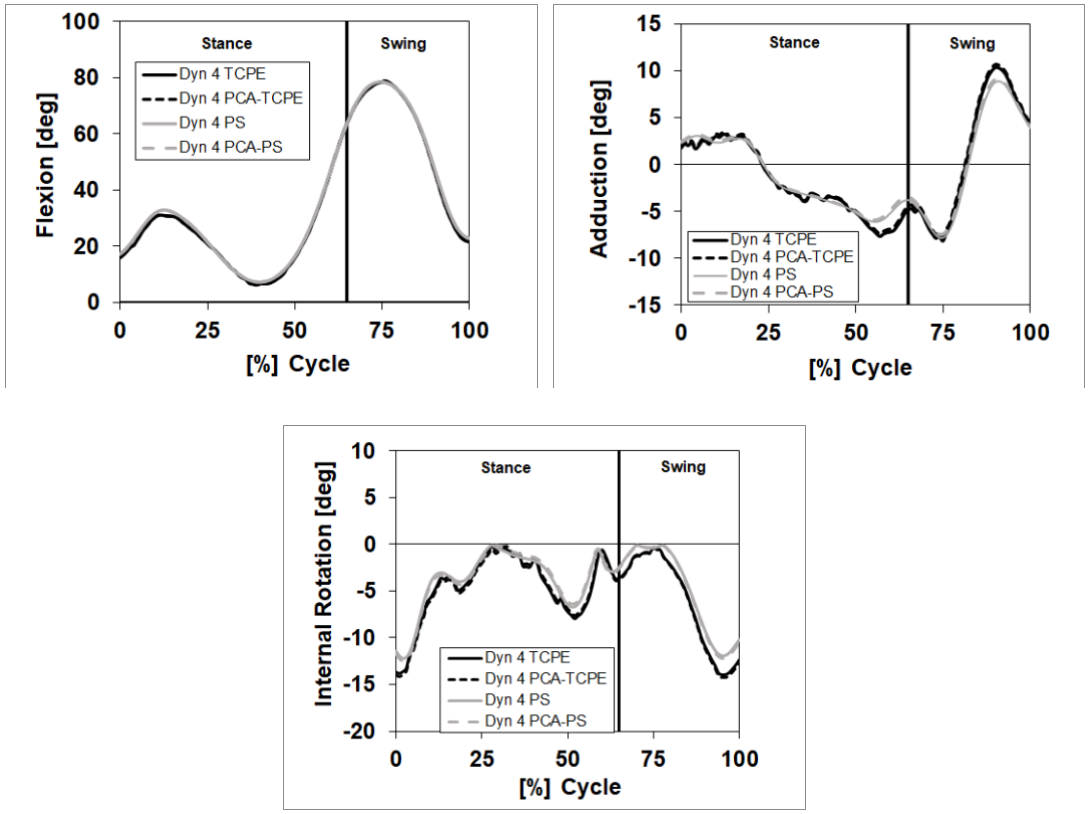

Figure D10: Trial 4 FE (top left), AA (top right) and IE (bottom) angles for participant 2.

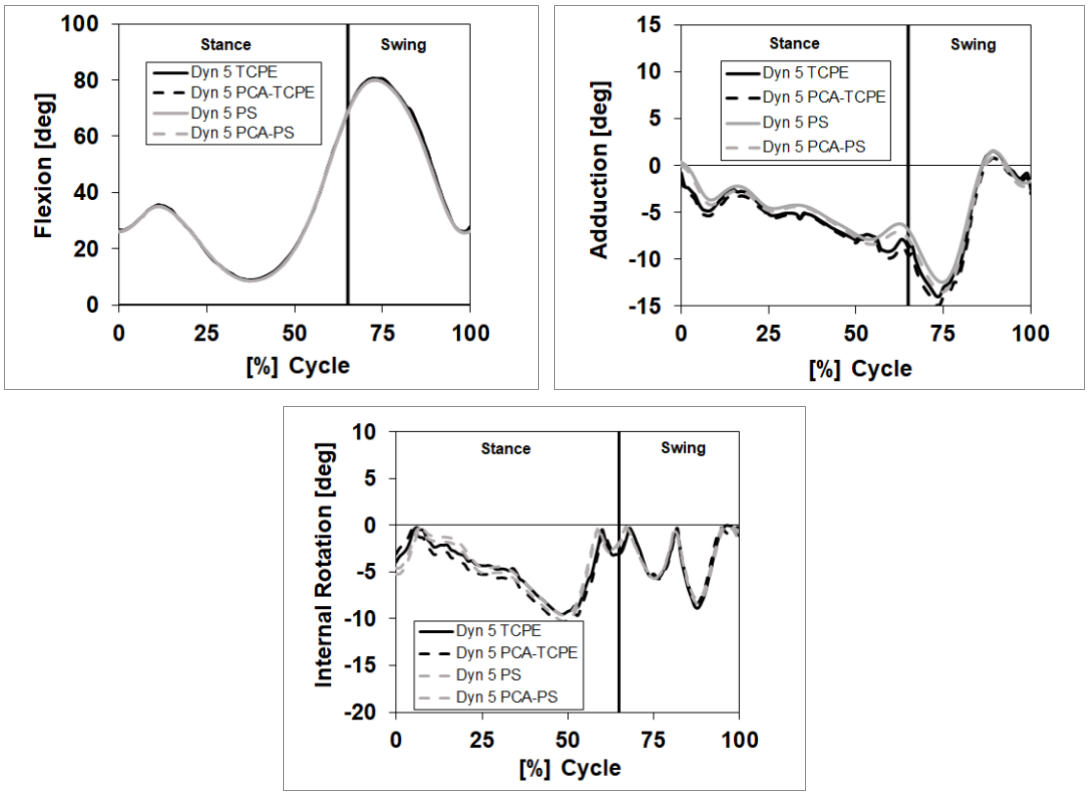

Figure D11: Trial 5 FE (top left), AA (top right) and IE (bottom) angles for participant 2.

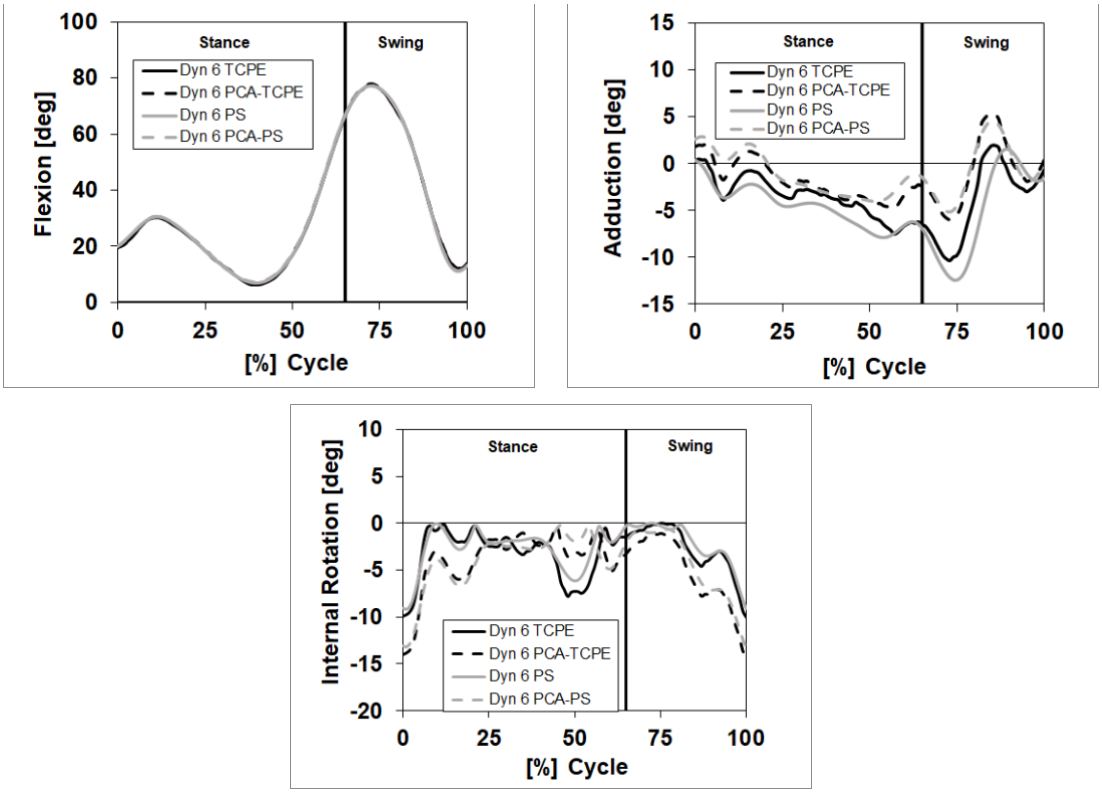

Figure D12: Trial 6 FE (top left), AA (top right) and IE (bottom) angles for participant 2.

APPENDIX E: FE-AA Plots Separated by Stance vs. Swing Phase

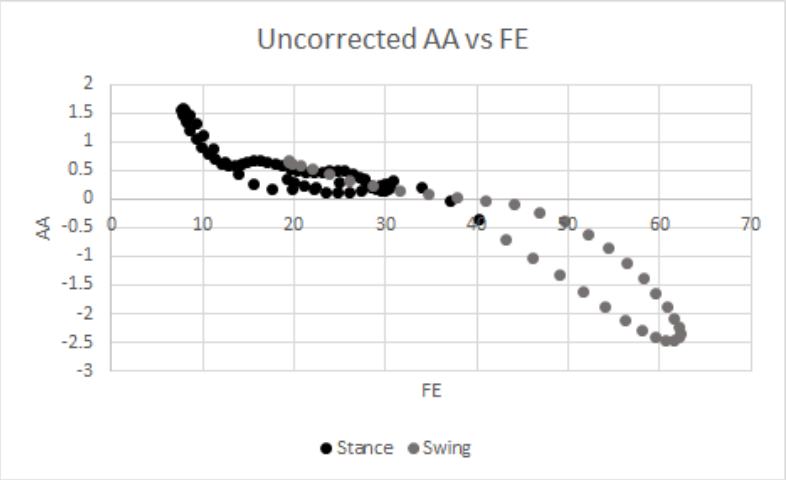

Figure E1: Average uncorrected FE-AA Plot for participant 1.

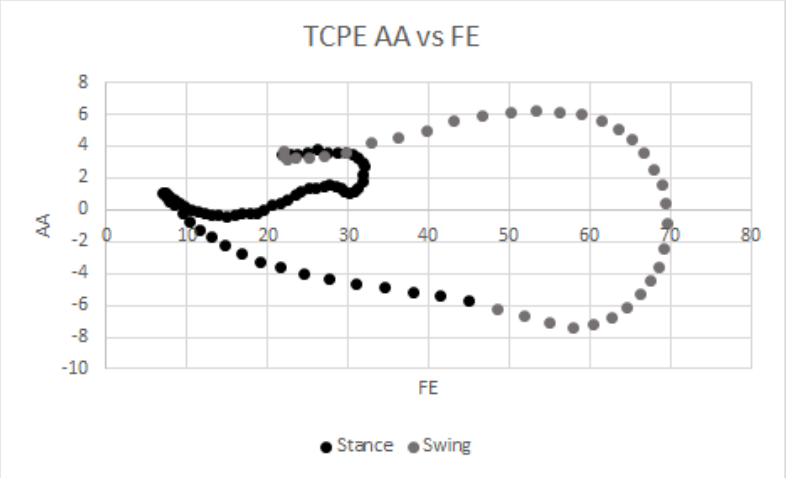

Figure E2: : Average TCPE FE-AA Plot for participant 1.

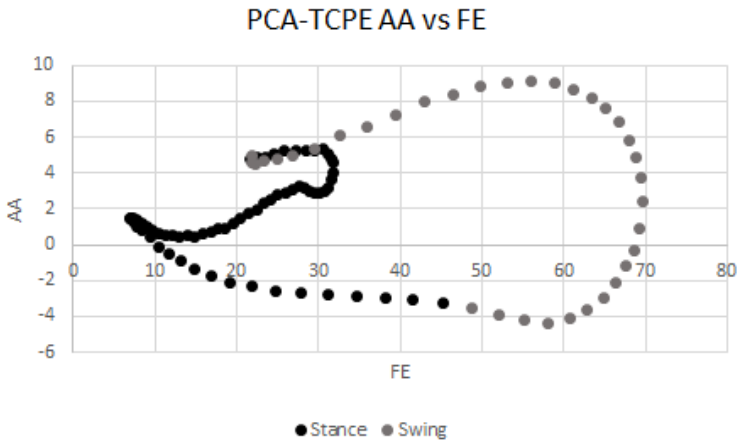

Figure E3: Average PCA-TCPE FE-AA Plot for participant 1.

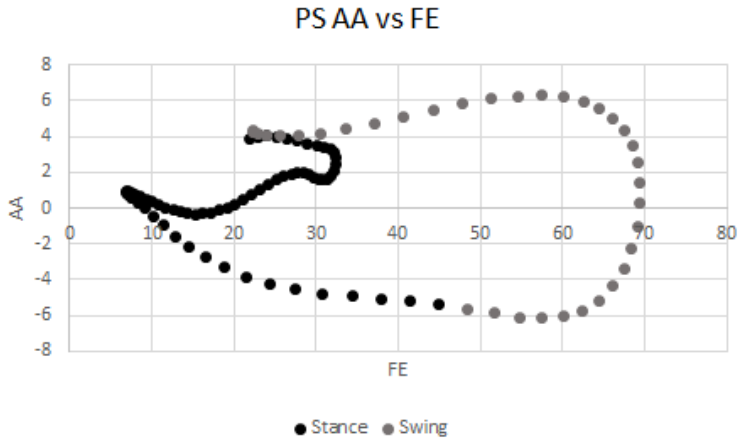

Figure E4: Average PS FE-AA Plot for participant 1.

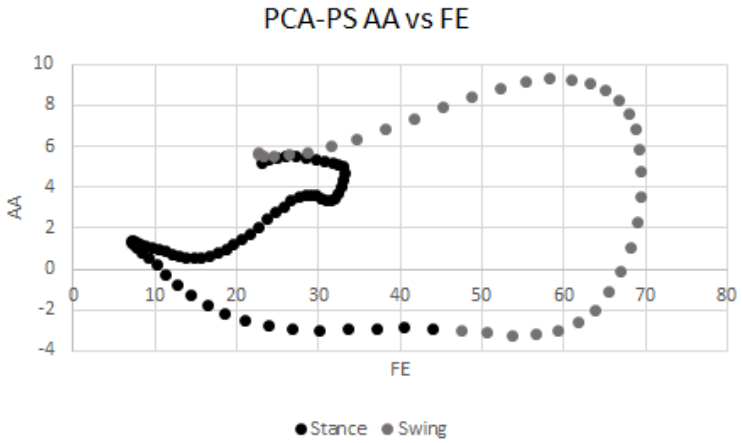

Figure E5: Average PCA-PS FE-AA Plot for participant 1.

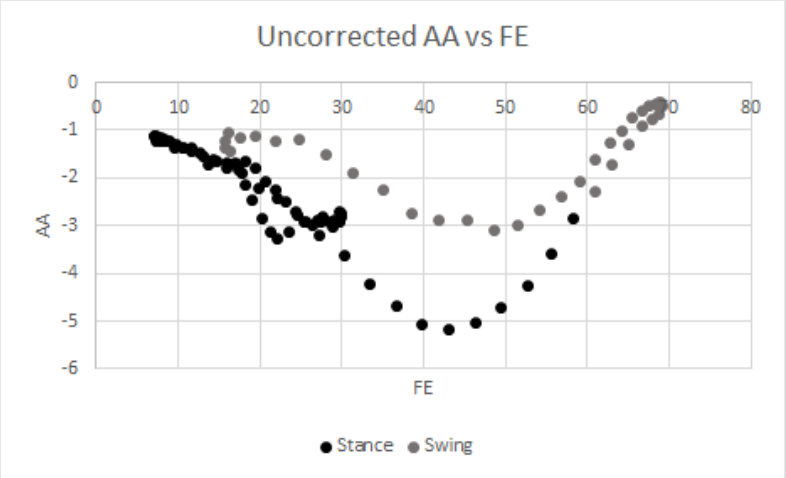

Figure E6: Average uncorrected FE-AA Plot for participant 2.

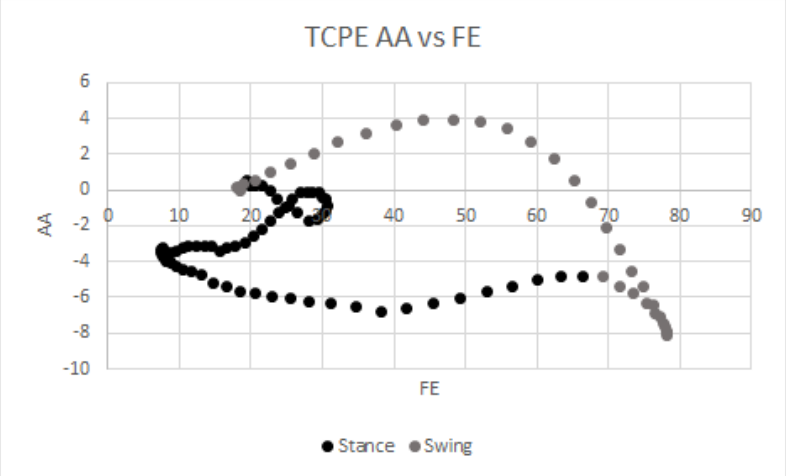

Figure E7: : Average TCPE FE-AA Plot for participant 2.

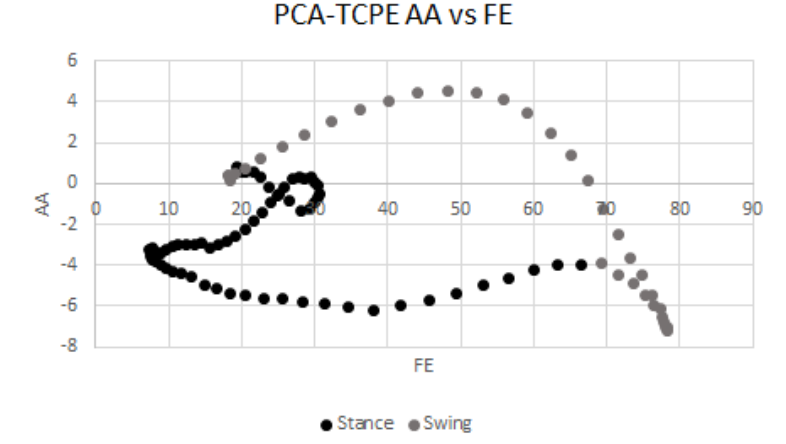

Figure E8: Average PCA-TCPE FE-AA Plot for participant 2.

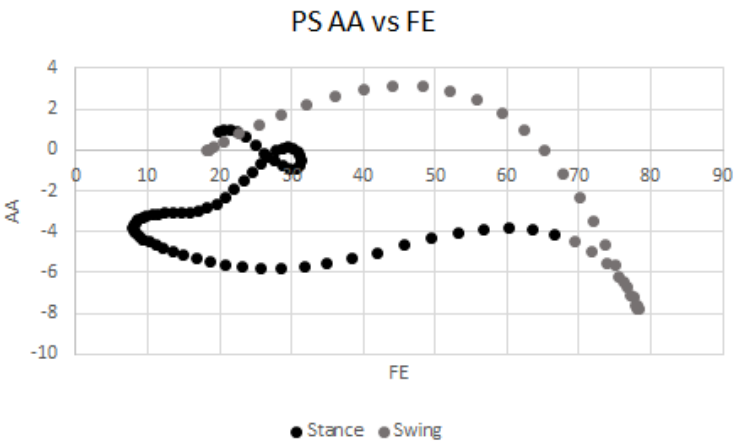

Figure E9: Average PS FE-AA Plot for participant 1.

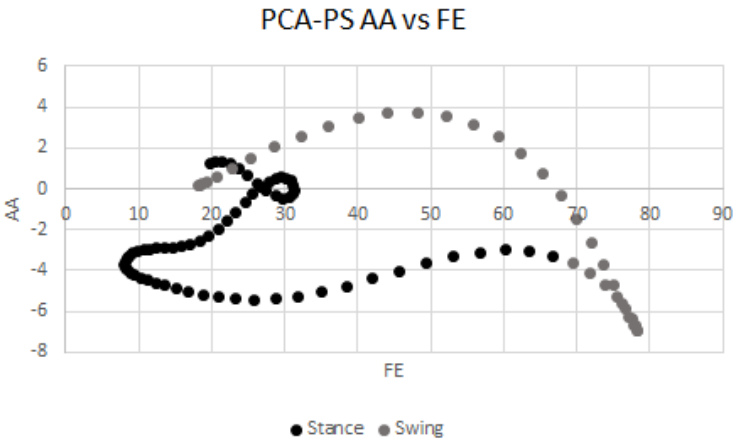

Figure E10: Average PCA-PS FE-AA Plot for participant 2.

APPENDIX F: Minitab Statistical Analyses Outputs

FLEXION-01

General Linear Model: RMSE versus Method, Trial

Method

Factor coding (-1, 0, +1)

Factor Information

Factor	Type	Levels	Values
Method	Fixed	3	PS-TCPE, UC-PS, UC-TCPE
Trial	Random	6	3, 4, 5, 12, 13, 14

Analysis of Variance

Source	DF	Adj SS	Adj MS	F-Value	P-Value
Method	2	44.4409	22.2204	531.66	0.000
Trial	5	0.8599	0.1720	4.11	0.027
Error	10	0.4179	0.0418		
Total	17	45.7187			

Model Summary

S	R-sq	R-sq(adj)	R-sq(pred)
0.204437	99.09%	98.45%	97.04%

Coefficients

Term	Coef	SE Coef	T-Value	P-Value	VIF
Constant	2.7991	0.0482	58.09	0.000	
Method					
PS-TCPE	-2.2181	0.0681	-32.55	0.000	1.33
UC-PS	1.2245	0.0681	17.97	0.000	1.33
Trial					
3	0.013	0.108	0.12	0.907	*
4	-0.017	0.108	-0.16	0.877	*
5	0.418	0.108	3.88	0.003	*
12	0.008	0.108	0.07	0.942	*
13	-0.105	0.108	-0.98	0.352	*

Tukey Pairwise Comparisons: Method

Grouping Information Using the Tukey Method and 95% Confidence

Method	N	Mean	Grouping
UC-PS	6	4.02362	A
UC-TCPE	6	3.79269	A
PS-TCPE	6	0.58096	B

Means that do not share a letter are significantly different.

Tukey Simultaneous Tests for Differences of Means

Difference of Method Levels	Difference of Means	SE of Difference	Simultaneous 95% CI	T-Value	Adjusted P-Value
UC-PS - PS-TCPE	3.443	0.169	(3.005, 3.880)	20.43	0.000
UC-TCPE - PS-TCPE	3.212	0.169	(2.774, 3.649)	19.06	0.000
UC-TCPE - UC-PS	-0.231	0.169	(-0.668, 0.206)	-1.37	0.380

Individual confidence level = 97.97%

Figure F1: Repeated measures and ANOVA and post-hoc Tukey test for Participant 1 FE

ABDUCTION-01

General Linear Model: RMSE versus Method, Trial

Method

Factor coding (-1, 0, +1)

Factor Information

Factor	Type	Levels	Values
Method	Fixed	3	PS-TCPE, UC-PS, UC-TCPE
Trial	Random	6	3, 4, 5, 12, 13, 14

Analysis of Variance

Source	DF	Adj SS	Adj MS	F-Value	P-Value
Method	2	35.085	17.5423	96.08	0.000
Trial	5	4.262	0.8523	4.67	0.019
Error	10	1.826	0.1826		
Total	17	41.172			

Model Summary

S	R-sq	R-sq(adj)	R-sq(pred)
0.427288	95.57%	92.46%	85.63%

Coefficients

Term	Coef	SE Coef	T-Value	P-Value	VIF	
Constant	2.636	0.101	26.18	0.000		
Method						
PS-TCPE	-1.974	0.142	-13.86	0.000	1.33	
UC-PS	1.007	0.142	7.07	0.000	1.33	
Trial						
3	0.024	0.225	0.11	0.916		*
4	-0.627	0.225	-2.78	0.019		*
5	0.507	0.225	2.25	0.048		*
12	0.329	0.225	1.46	0.175		*
13	0.447	0.225	1.98	0.075		*

Tukey Pairwise Comparisons: Method

Grouping Information Using the Tukey Method and 95% Confidence

Method	N	Mean	Grouping
UC-PS	6	3.64354	A
UC-TCPE	6	3.60366	A
PS-TCPE	6	0.66219	B

Means that do not share a letter are significantly different.

Tukey Simultaneous Tests for Differences of Means

Difference of Method Levels	Difference of Means	SE of Difference	Simultaneous 95% CI	T-Value	Adjusted P-Value
UC-PS - PS-TCPE	2.981	0.247	(2.305, 3.658)	12.09	0.000
UC-TCPE - PS-TCPE	2.941	0.247	(2.265, 3.618)	11.92	0.000
UC-TCPE - UC-PS	-0.040	0.247	(-0.717, 0.637)	-0.16	0.986

Individual confidence level = 97.93%

Figure F2: Repeated measures and ANOVA and post-hoc Tukey test for Participant 1 AA

INT ROT-01

General Linear Model: RMSE versus Method, Trial

Method

Factor coding (-1, 0, +1)

Factor Information

Factor	Type	Levels	Values
Method	Fixed	3	PS-TCPE, UC-PS, UC-TCPE
Trial	Random	6	3, 4, 5, 12, 13, 14

Analysis of Variance

Source	DF	Adj SS	Adj MS	F-Value	P-Value
Method	2	44.6869	22.3435	224.78	0.000
Trial	5	1.3043	0.2609	2.62	0.091
Error	10	0.9940	0.0994		
Total	17	46.9852			

Model Summary

S	R-sq	R-sq(adj)	R-sq(pred)
0.315282	97.88%	96.40%	93.15%

Coefficients

Term	Coef	SE Coef	T-Value	P-Value	VIF
Constant	3.0565	0.0743	41.13	0.000	
Method					
PS-TCPE	-2.228	0.105	-21.20	0.000	1.33
UC-PS	1.102	0.105	10.48	0.000	1.33
Trial					
3	-0.141	0.166	-0.85	0.415	*
4	-0.275	0.166	-1.66	0.129	*
5	0.452	0.166	2.72	0.022	*
12	0.258	0.166	1.55	0.152	*
13	-0.033	0.166	-0.20	0.845	*

Tukey Pairwise Comparisons: Method

Grouping Information Using the Tukey Method and 95% Confidence

Method	N	Mean	Grouping
UC-TCPE	6	4.18310	A
UC-PS	6	4.15804	A
PS-TCPE	6	0.82823	B

Means that do not share a letter are significantly different.

Tukey Simultaneous Tests for Differences of Means

Difference of Method Levels	Difference of Means	SE of Simultaneous Difference	95% CI	T-Value	Adjusted P-Value
UC-PS - PS-TCPE	3.330	0.182	(2.830, 3.829)	18.29	0.000
UC-TCPE - PS-TCPE	3.355	0.182	(2.855, 3.854)	18.43	0.000
UC-TCPE - UC-PS	0.025	0.182	(-0.474, 0.524)	0.14	0.990

Individual confidence level = 97.93%

Figure F3: Repeated measures and ANOVA and post-hoc Tukey test for Participant 1 IE

FLEXION-02

General Linear Model: RMSE versus Method, Trial

Method

Factor coding (-1, 0, +1)

Factor Information

Factor	Type	Levels	Values
Method	Fixed	3	PS-TCPE, UC-PS, UC-TCPE
Trial	Random	6	1, 2, 3, 4, 5, 6

Analysis of Variance

Source	DF	Adj SS	Adj MS	F-Value	P-Value
Method	2	77.12	38.560	17.07	0.001
Trial	5	41.04	8.209	3.63	0.039
Error	10	22.59	2.259		
Total	17	140.76			

Model Summary

S	R-sq	R-sq(adj)	R-sq(pred)
1.50315	83.95%	72.71%	47.99%

Coefficients

Term	Coef	SE Coef	T-Value	P-Value	VIF
Constant	3.673	0.354	10.37	0.000	
Method					
PS-TCPE	-2.927	0.501	-5.84	0.000	1.33
UC-PS	1.506	0.501	3.01	0.013	1.33
Trial					
1	-0.706	0.792	-0.89	0.394	*
2	-0.545	0.792	-0.69	0.507	*
3	-0.973	0.792	-1.23	0.248	*
4	-0.712	0.792	-0.90	0.390	*
5	-0.419	0.792	-0.53	0.608	*

Tukey Pairwise Comparisons: Method

Grouping Information Using the Tukey Method and 95% Confidence

Method	N	Mean	Grouping
UC-PS	6	5.17895	A
UC-TCPE	6	5.09329	A
PS-TCPE	6	0.74585	B

Means that do not share a letter are significantly different.

Tukey Simultaneous Tests for Differences of Means

Difference of Method Levels	Difference of Means	SE of Difference	Simultaneous 95% CI	T-Value	Adjusted P-Value
UC-PS - PS-TCPE	4.433	0.868	(2.052, 6.814)	5.11	0.001
UC-TCPE - PS-TCPE	4.347	0.868	(1.966, 6.728)	5.01	0.001
UC-TCPE - UC-PS	-0.086	0.868	(-2.467, 2.295)	-0.10	0.995

Individual confidence level = 97.93%

Figure F4: Repeated measures and ANOVA and post-hoc Tukey test for Participant 2 FE

ABDUCTION-02

General Linear Model: RMSE versus Method, Trial

Method

Factor coding (-1, 0, +1)

Factor Information

Factor	Type	Levels	Values
Method	Fixed	3	PS-TCPE, UC-PS, UC-TCPE
Trial	Random	6	1, 2, 3, 4, 5, 6

Analysis of Variance

Source	DF	Adj SS	Adj MS	F-Value	P-Value
Method	2	41.934	20.9668	62.82	0.000
Trial	5	9.858	1.9716	5.91	0.009
Error	10	3.338	0.3338		
Total	17	55.129			

Model Summary

S	R-sq	R-sq(adj)	R-sq(pred)
0.577725	93.95%	89.71%	80.38%

Coefficients

Term	Coef	SE Coef	T-Value	P-Value	VIF	
Constant	2.962	0.136	21.75	0.000		
Method						
PS-TCPE	-2.154	0.193	-11.19	0.000	1.33	
UC-PS	0.961	0.193	4.99	0.001	1.33	
Trial						
1	-0.280	0.304	-0.92	0.380		*
2	-1.202	0.304	-3.95	0.003		*
3	-0.460	0.304	-1.51	0.162		*
4	0.793	0.304	2.61	0.026		*
5	0.936	0.304	3.07	0.012		*

Tukey Pairwise Comparisons: Method

Grouping Information Using the Tukey Method and 95% Confidence

Method	N	Mean	Grouping
UC-TCPE	6	4.15562	A
UC-PS	6	3.92329	A
PS-TCPE	6	0.80791	B

Means that do not share a letter are significantly different.

Tukey Simultaneous Tests for Differences of Means

Difference of Method Levels	Difference of Means	SE of Difference	Simultaneous 95% CI	T-Value	Adjusted P-Value
UC-PS - PS-TCPE	3.115	0.334	(2.200, 4.031)	9.34	0.000
UC-TCPE - PS-TCPE	3.348	0.334	(2.433, 4.263)	10.04	0.000
UC-TCPE - UC-PS	0.232	0.334	(-0.683, 1.147)	0.70	0.771

Individual confidence level = 97.93%

Figure F5: Repeated measures and ANOVA and post-hoc Tukey test for Participant 2 AA

INT ROT-02

General Linear Model: RMSE versus Method, Trial

Method

Factor coding (-1, 0, +1)

Factor Information

Factor	Type	Levels	Values
Method	Fixed	3	PS-TCPE, UC-PS, UC-TCPE
Trial	Random	6	1, 2, 3, 4, 5, 6

Analysis of Variance

Source	DF	Adj SS	Adj MS	F-Value	P-Value
Method	2	141.19	70.596	35.24	0.000
Trial	5	32.38	6.476	3.23	0.054
Error	10	20.03	2.003		
Total	17	193.60			

Model Summary

S	R-sq	R-sq(adj)	R-sq(pred)
1.41533	89.65%	82.41%	66.48%

Coefficients

Term	Coef	SE Coef	T-Value	P-Value	VIF	
Constant	5.096	0.334	15.28	0.000		
Method						
PS-TCPE	-3.945	0.472	-8.36	0.000	1.33	
UC-PS	1.670	0.472	3.54	0.005	1.33	
Trial						
1	-1.460	0.746	-1.96	0.079		*
2	-1.773	0.746	-2.38	0.039		*
3	-0.140	0.746	-0.19	0.855		*
4	0.662	0.746	0.89	0.396		*
5	0.524	0.746	0.70	0.499		*

Tukey Pairwise Comparisons: Method

Grouping Information Using the Tukey Method and 95% Confidence

Method	N	Mean	Grouping
UC-TCPE	6	7.37133	A
UC-PS	6	6.76547	A
PS-TCPE	6	1.15041	B

Means that do not share a letter are significantly different.

Tukey Simultaneous Tests for Differences of Means

Difference of Method Levels	Difference of Means	SE of Difference	95% CI	T-Value	Adjusted P-Value
UC-PS - PS-TCPE	5.615	0.817	(3.373, 7.857)	6.87	0.000
UC-TCPE - PS-TCPE	6.221	0.817	(3.979, 8.463)	7.61	0.000
UC-TCPE - UC-PS	0.606	0.817	(-1.636, 2.848)	0.74	0.745

Individual confidence level = 97.93%

Figure F6: Repeated measures and ANOVA and post-hoc Tukey test for Participant 2 IE

RM ANOVA

General Linear Model: R^2 versus Trial, Method

Method

Factor coding (-1, 0, +1)

Factor Information

Factor	Type	Levels	Values
Trial	Random	6	3, 4, 5, 12, 13, 14
Method	Fixed	4	PCA-PS, PCA-TCPE, PS, TCPE

Analysis of Variance

Source	DF	Adj SS	Adj MS	F-Value	P-Value
Trial	5	0.042116	0.008423	2.46	0.081
Method	3	0.002883	0.000961	0.28	0.838
Error	15	0.051299	0.003420		
Total	23	0.096298			

Model Summary

S	R-sq	R-sq(adj)	R-sq(pred)
0.0584801	46.73%	18.32%	0.00%

Coefficients

Term	Coef	SE Coef	T-Value	P-Value	VIF
Constant	0.0474	0.0119	3.97	0.001	
Trial					
3	0.0068	0.0267	0.26	0.802	*
4	-0.0135	0.0267	-0.51	0.619	*
5	-0.0289	0.0267	-1.08	0.296	*
12	-0.0327	0.0267	-1.23	0.239	*
13	-0.0208	0.0267	-0.78	0.447	*
Method					
PCA-PS	0.0176	0.0207	0.85	0.408	1.50
PCA-TCPE	-0.0103	0.0207	-0.50	0.624	1.50
PS	-0.0079	0.0207	-0.38	0.707	1.50

Tukey Pairwise Comparisons: Method

Grouping Information Using the Tukey Method and 95% Confidence

Method	N	Mean	Grouping
PCA-PS	6	0.0650333	A
TCPE	6	0.0480667	A
PS	6	0.0394833	A
PCA-TCPE	6	0.0370833	A

Means that do not share a letter are significantly different.

Tukey Simultaneous Tests for Differences of Means

Difference of Method Levels	Difference of Means	SE of Difference	Simultaneous 95% CI	T-Value	Adjusted P-Value
PCA-TCPE - PCA-PS	-0.0280	0.0338	(-0.1254, 0.0695)	-0.83	0.840
PS - PCA-PS	-0.0255	0.0338	(-0.1230, 0.0719)	-0.76	0.872
TCPE - PCA-PS	-0.0170	0.0338	(-0.1144, 0.0804)	-0.50	0.957
PS - PCA-TCPE	0.0024	0.0338	(-0.0950, 0.0998)	0.07	1.000
TCPE - PCA-TCPE	0.0110	0.0338	(-0.0864, 0.1084)	0.33	0.988
TCPE - PS	0.0086	0.0338	(-0.0888, 0.1060)	0.25	0.994

Individual confidence level = 98.87%

Figure F7: Repeated measures and ANOVA and post-hoc Tukey test for Participant 1 PCA FE-AA Correlations for TCPE, PS, PCA-TCPE and PCA-PS

RM ANOVA-02

General Linear Model: R^2 versus Trial, Method

Method

Factor coding (-1, 0, +1)

Factor Information

Factor	Type	Levels	Values
Trial	Random	6	1, 2, 3, 4, 5, 6
Method	Fixed	4	PCA-PS, PCA-TCPE, PS, TCPE

Analysis of Variance

Source	DF	Adj SS	Adj MS	F-Value	P-Value
Trial	5	0.174041	0.034808	13.50	0.000
Method	3	0.005253	0.001751	0.68	0.578
Error	15	0.038677	0.002578		
Total	23	0.217971			

Model Summary

S	R-sq	R-sq(adj)	R-sq(pred)
0.0507785	82.26%	72.79%	54.58%

Coefficients

Term	Coef	SE Coef	T-Value	P-Value	VIF
Constant	0.0646	0.0104	6.23	0.000	
Trial					
1	-0.0390	0.0232	-1.68	0.113	*
2	-0.0633	0.0232	-2.73	0.015	*
3	-0.0573	0.0232	-2.47	0.026	*
4	-0.0527	0.0232	-2.27	0.038	*
5	0.1746	0.0232	7.54	0.000	*
Method					
PCA-PS	-0.0135	0.0180	-0.75	0.464	1.50
PCA-TCPE	-0.0160	0.0180	-0.89	0.388	1.50
PS	0.0130	0.0180	0.73	0.479	1.50

Tukey Pairwise Comparisons: Method

Grouping Information Using the Tukey Method and 95% Confidence

Method	N	Mean	Grouping
TCPE	6	0.0810018	A
PS	6	0.0776500	A
PCA-PS	6	0.0511167	A
PCA-TCPE	6	0.0486500	A

Means that do not share a letter are significantly different.

Tukey Simultaneous Tests for Differences of Means

Difference of Method Levels	Difference of Means	SE of Difference	Simultaneous 95% CI	T-Value	Adjusted P-Value
PCA-TCPE - PCA-PS	-0.0025	0.0293	(-0.0870, 0.0821)	-0.08	1.000
PS - PCA-PS	0.0265	0.0293	(-0.0580, 0.1111)	0.91	0.802
TCPE - PCA-PS	0.0299	0.0293	(-0.0547, 0.1145)	1.02	0.741
PS - PCA-TCPE	0.0290	0.0293	(-0.0556, 0.1136)	0.99	0.758
TCPE - PCA-TCPE	0.0324	0.0293	(-0.0522, 0.1169)	1.10	0.693
TCPE - PS	0.0034	0.0293	(-0.0812, 0.0879)	0.11	0.999

Individual confidence level = 98.87%

Figure F8: Repeated measures and ANOVA and post-hoc Tukey test for Participant 2 PCA FE-AA Correlations for TCPE, PS, PCA-TCPE and PCA-PS